transplantation depended on the kind of *AML1* mutants used in this study and on the integration sites of retroviruses. Considering the recent reports of the effects of retrovirus integration sites on biological results,[30-38] identification of integration sites may lead to the discovery of the genes involved in the induction of MDS/AML in concert with *AML1* mutants. Intriguingly, the enhanced expression of Evi1 by retrovirus integration seemed to collaborate with AML1-D171N to induce MDS/AML with the same phenotype. Moreover, we confirmed that combination of AML1-D171N and *Evi1* induced AML of the same phenotype with shorter latencies in the mouse BMT model. This model will allow valuable insight into the molecular pathogenesis of MDS and MDS/AML.

Methods

Vector construction

We used 2 *AML1* mutants, D171N or S291fsX300, identified from case no. 5 or 27, respectively, among patients with MDS/AML.[25,26] These mutants are hereafter referred to as AML1-D171N and AML1-S291fs. AML1 wild-type (WT; AML1b), AML1-D171N, or AML1-S291fs, which was fused with a FLAG epitope tag at the N-terminus, was inserted upstream of the IRES-EGFP cassette of pMYs-IG to generate pMYs-AML1 WT, D171N, or S291fs-IG, respectively. pMYs-mouse Evi1-IG were kindly provided by Dr T. Nakamura (The Cancer Institute, Tokyo, Japan).[38]

Transfection and retrovirus production

Plat-E[39] packaging cells maintained in Dulbecco modified Eagle medium (DMEM) supplemented with 10% fetal calf serum (FCS) were transfected with retroviral constructs by using FuGENE 6 (Roche Diagnostics, Mannheim, Germany) according to the manufacturer's recommendations. The medium was changed 1 day after the transfection, and retroviruses were harvested 48 hours after the transfection as previously described.[39,40] Titers of the retroviruses were assessed based on the number of neomycin-resistant colonies of the infected NIH3T3 cells (average: 10^7 infection U/mL) as described.[39]

Mouse BMT

Bone marrow mononuclear cells were isolated from the femurs and tibias of C57BL/6 (Ly-5.1) donor mice (9-12 weeks of age) 4 days after intraperitoneal administration of 150 mg/kg 5-fluorouracil (5-FU) and cultured overnight in α minimal essential medium (αMEM) supplemented with 20% FCS and 50 ng/mL of mouse stem cell factor (SCF), mouse FLT3 ligand (FL), human IL-6, and human thrombopoietin (TPO; R&D Systems, Minneapolis, MN). The prestimulated cells were infected for 60 hours with the retroviruses harboring pMYs-AML1 WT, D171N, or S291fs-IG, or an empty vector as a control, using 6-well dishes coated with RetroNectin (Takara Bio, Shiga, Japan) according to the manufacturer's recommendations. Then, 0.2 to 3.5 × 10^6 of infected bone marrow cells (Ly-5.1) were injected through tail vein into C57BL/6 (Ly-5.2)–recipient mice (8-12 weeks of age) which had been administered a sublethal dose of 5.25 Gy or a lethal dose of 9.5 Gy total-body γ-irradiation (^{135}Cs). For the lethally irradiated mice, a radioprotective dose of 2 × 10^5 of bone marrow cells (Ly-5.2) was simultaneously injected. Probabilities of overall survival of the mice that received transplants were estimated using the Kaplan-Meier method. All animal studies were approved by the Animal Care Committee of the Institute of Medical Science, The University of Tokyo.

Analysis of the mice that underwent transplantation

Engraftment of bone marrow cells infected with retroviruses was confirmed by measuring the percentage of GFP$^+$ and Ly-5.1$^+$ cells in peripheral blood obtained every 1 to 2 months after the transplantation.

After the morbid mice were killed, their tissue samples, including peripheral blood (PB), bone marrow (BM), spleen, liver, and kidney, were analyzed. Circulating blood cells were counted by an analyzer. Morphology of the peripheral blood was evaluated by staining of air-dried smears with Hemacolor (Merck, Darmstadt, Germany). Tissues were fixed in 10% buffered formalin, embedded in paraffin, sectioned, and stained with hematoxylin and eosin (H&E). Cytospin preparations of bone marrow and spleen cells were also stained with Hemacolor. Percentage of blasts, myelocytes, neutrophils, monocytes, lymphocytes, and erythroblasts was estimated by examination of at least 200 cells. To assess whether the leukemic cells were transplantable, 2 × 10^5 to 10^6 total BM cells including blasts were injected into the tail veins of sublethally irradiated mice. A total of 2 or 3 recipient mice were used for each serial transplantation.

Flow cytometric analysis

Red blood cells were lysed by using Ammonium Chloride Lysing Reagent (BD Biosciences, San Jose, CA) in PB or single-cell suspensions of bone marrow and spleen. Washed cells were incubated for 15 minutes at 4°C with 2.4G2 antibody for blocking and then stained for 20 minutes at 4°C with the following monoclonal phycoerythrin (PE)–conjugated antibodies: Ly-5.1, Gr-1, CD11b, B220, CD3, CD41, c-Kit, Sca-1, CD34, and Ter119. Flow cytometric analysis of the stained cells was performed with FACSCalibur flow (BD Biosciences) equipped with CellQuest software (BD Biosciences) and Flowjo software (Tree Star, San Carlos, CA).

Diagnosis

Diagnosis was made according to the Bethesda proposals for classification of nonlymphoid hematopoietic neoplasms in mice.[41]

Real-time RT-PCR

Total RNA was extracted from BM cells using Trizol (Invitrogen, Carlsbad, CA). cDNA was prepared with the Superscript II RT kit (Invitrogen). Real-time reverse transcription–polymerase chain reaction (RT-PCR) was performed using a LightCycler Workflow System (Roche Diagnostics). cDNA was amplified using a SYBR Premix EX Taq (TAKARA). Reaction was subject to one cycle of 95°C for 30 seconds, 45 cycles of PCR at 95°C for 5 seconds, 55°C for 10 seconds, and 72°C for 10 seconds. All samples were independently analyzed at least 3 times. The following primer pairs were used: 5′-CCAGATGTCACATGACAGTGGAAAGCACTA-3′ (forward) and 5′-CCGGGTTGGCATGACTCATATTAACCATGG-3′ (reverse) for Evi1; 5′-TACCTCAACCCCTGACAGCTATGG-3′ (forward) and 5′-TCGGTTGGAGATATCAGAGTGCAG-3′ (reverse) for MN1;[42] and 5′-GTTATCCCATCTGCATCAGCATCTGG-3′ (forward) and 5′-GGTCCTCTTCACTCTTCATGAACAGC-3′ (reverse) for MDS1/Evi1.[43] Relative gene expression levels were calculated using standard curves generated by serial dilutions of cDNA. Product quality was checked by melting curve analysis via LightCycler software (Roche Diagnostics). Expression levels were normalized by a control, the expression level of GAPDH mRNA.

Western blot analysis

To detect the expression of *AML1* WT, mutants, or *Evi1*, equal numbers of spleen cells were lysed, and Western blotting was performed as described with minor modifications.[13] Polyclonal rabbit anti-Evi1 antibody (a kind gift from Dr M. Kurokawa, Tokyo University, Tokyo, Japan), or a monoclonal mouse anti-Flag antibody (Sigma-Aldrich, St Louis, MO) was used for *Evi1* or *AML1*, respectively.

Southern blot analysis

Genomic DNA was extracted from BM or spleen cells. After enzymatic digestion of 10 μg DNA with *Eco*RI followed by electrophoretic separation, proviruses were probed with a GFP probe.

Bubble PCR

A total of 10 μg of genomic DNA extracted from BM or spleen cells was digested with *Eco*RI, and the fragments were ligated overnight at 16°C to a double-stranded bubble linker (5′-AATTGAAGGAGAGGACGCTGTCTG-

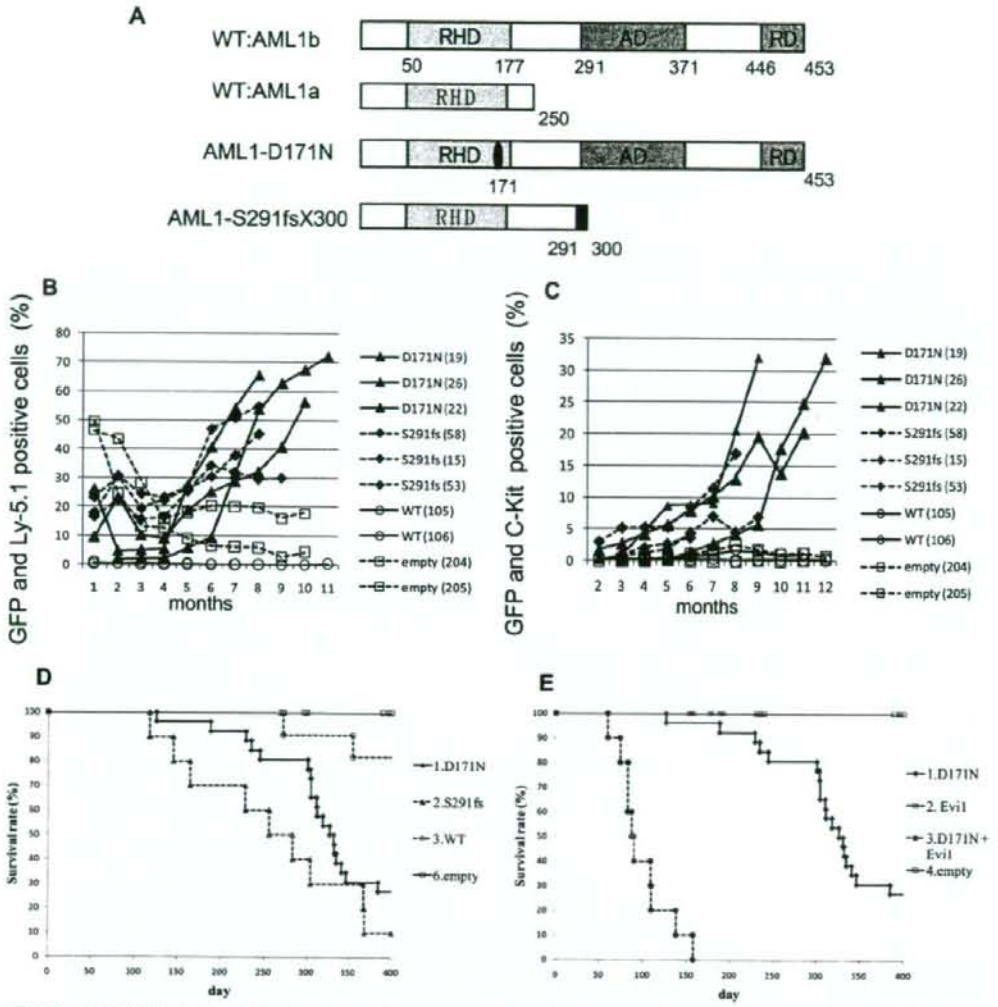

Figure 1. MDS and MDS/AML induced by *AML1* mutants derived from patients with MDS. (A) Schematics of *AML1* WT (AML1a and AML1b) and *AML1* mutants (D171N and S291fs). AD indicates transactivating domain; RD, repression domain. (B) Percentages of GFP/Ly-5.1 double-positive cells or (C) c-Kit$^+$ cells in PB. PB was obtained from the tail vein every month after the transplantation. Numbers in parenthesis indicate mouse IDs. (D) Kaplan-Meier analysis for the survival of mice that received transplants of *AML1* mutant-transduced BM cells. Average survival days of AML1-D171N (340.6 days) were compared with AML1-S291fs (263.6 days) using the log-rank test; $P = .218$. AML1 WT (n = 11), D171N (n = 26), S291fs (n = 10), mock (n = 16). (E) Evi1 synergized with AML1-D171N in inducing MDS/AML. D171N (n = 26; same as those in panel D), *Evi1* (n = 8), D171N + *Evi1* (n = 10), and mock (n = 16) transduced bone marrow cells were transplanted into mice.

TCGAAGGTAAGGAACGGACGAGAGAAGGGAGAG-3′ and 5′-GACTC-TCCCTTCTCGAATCGTAACCGTTCGTACGAGAATCGCTGTCCTCTCC-TTC-3′).[44] Next, PCR was performed on the ligation product using a linker-specific Vectorette primer (5′-CGAATCGTAACCGTTCGTACGAGAATCGCT-3′)[44,45] and a long-terminal repeat (LTR)–specific primer (5′-CGAGCTCAATAAAA-GAGCCCACAACCCC-3′) under the following conditions: one cycle of 95°C for 5 minutes, 10 cycles of 95°C for 30 seconds, and 67°C for 30 seconds and 72°C for 3 minutes, 10 cycles of 95°C for 30 seconds, and 67°C (this annealing temperature was reduced by 1°C each cycle) for 30 seconds and 72°C for 3 minutes, 15 cycles of 95°C for 30 seconds and 57°C for 30 seconds and 72°C for 3 minutes, and one cycle of 72°C for 90 seconds. Next, nested PCR was performed on 2 μL of PCR products using a linker-specific Vectorette primer and an LTR-specific primer (5′-ATAAAAGAGCCCACAACCCCTCACTCGG-3′) under the following conditions: 1 cycle of 95°C for 5 minutes, 35 cycles of 95°C for 30 seconds and 60°C for 30 seconds and 72°C for 3 minutes, and 1 cycle of 72°C for 90 seconds. The PCR product was electrophoresed using 1.0% agarose gel. Individual bands were excised and purified using PCR clear (Promega, Madison, WI) and were sequenced to identify the integration site of retrovirus. We confirmed inverse repeat sequence "GGGGGTCTTTCA" as a marker of junction between genomic DNA and retrovirus sequence.

Results

The ratio of *AML1* mutant-transduced cells gradually increased over several months after transplantation

To examine the effect of *AML1* mutants on the hematopoietic abnormality, we chose 2 distinct mutants, AML1-D171N and AML1-S291fsX300, which are found in patients with MDS/

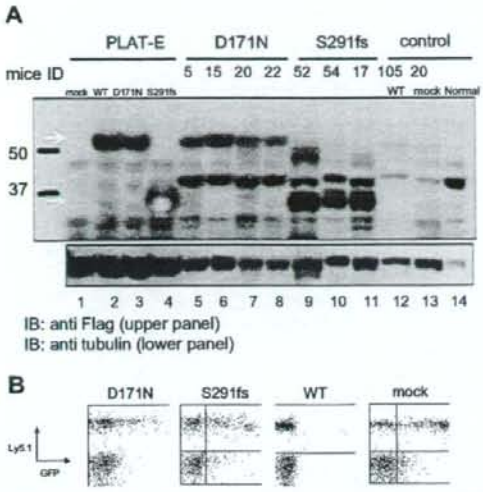

Figure 2. Expression of the transduced AML1-D171N, AML1-S291fs, and AML1 WT in spleen of the transplanted mice. (A) Lysates of spleen cells were immunoblotted with anti-Flag Ab. As a positive control, Plat-E packaging cells were transduced with mock (lane 1), AML1 WT (lane 2), AML1-D171N (lane 3), or AML1-S291fs (lane 4). Spleen cells were derived from mice/D171N (lanes 5-8), mice/S291fs (lanes 9-11), mice/WT (lane 12), mice/mock (lane 13), or control normal mouse (lane 14). White arrows indicate transduced AML1 WT, AML1-D171N, and AML1-S291fs. (B) AML1 WT-transduced cells were undetectable in PB at 1 month after the transplantation. Flow cytometric analysis of PB obtained from mice that received transplants of AML1-D171N, AML1-S291fs, AML1 WT, and mock at 1 month after transplantation.

AML.[25,26] The former has a point mutation in RHD, and the latter possesses a frameshift mutation in the C-terminal region, resulting in truncation of the authentic protein (Figure 1A). Ly-5.1 murine BM cells infected with retroviruses harboring AML1 WT, AML1-D171N, AML1-S291fsX300, or empty vector were transplanted into irradiated syngeneic Ly-5.2 mice. In most of mice that received transplants of AML1-D171N– or S291fsX300-transduced cells (hereafter referred to as mice/D171N or mice/S291fs, respectively), the ratio of GFP$^+$ and Ly-5.1$^+$ cells gradually increased over several months after the transplantation (Figure 1B), but not in mice that received transplants of AML1 WT-transduced cells or control retrovirus-infected cells (hereafter referred to as mice/WT or mice/mock, respectively). Gradual increase of c-kit$^+$ cells in the PB was also observed in the mice that received transplants of *AML1* mutant-transduced cells during the observation period (Figure 1C). Cells positive for c-kit and GFP—that is, c-kit$^+$ cells transduced with *AML1* mutants—were morphologically blasts with high nuclear-cytoplasmic ratios (data not shown). In fact, the percentage of blasts gradually increased in the PB of the mice that received transplants of *AML1* mutant-transduced cells, especially the mice/D171N. Finally, most of mice/D171N or mice/S291fs became sick and died with latencies of 4 to 13 months after the transplantation, while mice/mock were healthy over the observation period (Figure 1D). Overall survival of mice/D171N was not significantly different from that of mice/S291fs ($P = .218$). Expression of the transduced AML1-D171N or AML1-S291fs in spleen cells was confirmed by Western blot analysis (Figure 2A). Two of the mice/WT died during the observation period. BM of the 2 mice was occupied with GFP/Ly5.1 double-negative cells. One of the mice/WT developed leukemia derived from recipient cells at 272 days after transplantation. The remaining one mouse/WT died of anemia with unknown reason at 355 days after transplantation.

Interestingly, in the peripheral blood of mice/WT, GFP$^+$ cell counts were extremely low 1 month after transplantation and thereafter became undetectable, despite the fact that 14% to 27% of the BM cells were positive for GFP before transplantation (Figures 1B,2B; Table S1, available on the *Blood* website; see the Supplemental Materials link at the top of the online article). Consistently, the expression of transduced AML1 WT was not detected in spleen cells of mice/WT (Figure 2A; mouse ID: 105). These data suggested that forced expression of AML1 WT in the stem cells had a negative effect on the survival and expansion of these cells in the BM. Recently, Tsuzuki et al reported that expression of the full-length isoform AML1b abrogated engraftment potential of murine long-term reconstituting stem cells in a mouse BMT model.[46] Their result coincides with our result.

AML1-D171N and AML1-S291fs induced different diseases in mice that underwent transplantation

PB cell counts were different between mice/D171N and mice/S291fs; most mice/D171N (Figure 3A; lanes 1,2) showed leukocytosis, while mice/S291fs (Figure 3A; lane 3) showed leukocytopenia. This difference was significant ($P = .007$). Macroscopic observation of morbid mice revealed that severe hepatosplenomegaly was exclusively found in mice/D171N, but not in mice/S291fs (Figure 3E,F; Table S2).

The smear specimens of peripheral blood were obtained every 1 to 2 months. The specimens showed that most of mice/D171N and mice/S291fs suffered from multilineage dysplasia characteristic of MDS. Erythroid dysplasia such as Howell-Jolly bodies, red cell polychromasia, and poikilocytosis (Figure 4A) were frequently detected in both mice. In BM specimens of morbid mice, orthochromatic giant erythroblasts and karyorrhexis were detected (Figure 4B). Erythroid dysplasia was more evident in mice/S291fs than in mice/D171N. As recently described in a mouse MDS model,[15] increase of red blood cell mean corpuscular volume (MCV) was also observed in most mice/D171N and mice/S291fs (Figure 3D; Table S2). Myeloid dysplasia such as the pseudo–Pelger-Huet anomaly (Figure 4C) was frequently detected in mice/D171N. Hypersegmented neutrophils (Figure 4D) and giant platelets (Figure 4F) were observed in 2 mice/D171N (mouse IDs 9 and 17). Collectively, *AML1* mutants used in this study induced multilineage dysplasia, in particular in erythroid and myeloid lineages. Continuous pancytopenia was observed in 7 of 8 morbid mice/S291fs and 2 of 16 morbid mice/D171N, although BM of the morbid mice was not hypocellular but hypercellular or normocellular. Based on these findings, a final diagnosis was made by the ratio of blasts in the bone marrow according to the Bethesda proposals for classification of nonlymphoid hematopoietic neoplasms in mice.[41] As a result, MDS/AML was recognized in 13 of 16 morbid mice/D171N and in 5 of 8 morbid mice/S291fs, while MDS-RAEB was recognized in 2 of 16 morbid mice/D171N and 2 of 8 morbid mice/S291fs (Table S2). One mouse/D171N was diagnosed with AML at 4 months after transplantation because we did not examine to see if the MDS phase had preceded AML (mouse ID 5). The leukemic cells derived from either mice/D171N or mice/S291fs were serially transplantable. We confirmed the serial transplantability in 11 mice/D171N (mouse IDs 4, 6, 9, 12-15, 17, 20, 22, and 26) and 6 mice/S291fs (mouse IDs 52, 54-56, 58, and 60). Penetrance of serial transplantation was 100%, except for mouse IDs 9 and 17; that is, 33% and 50%, respectively. Mice that underwent serial transplantation showed more aggressive status than primary mice

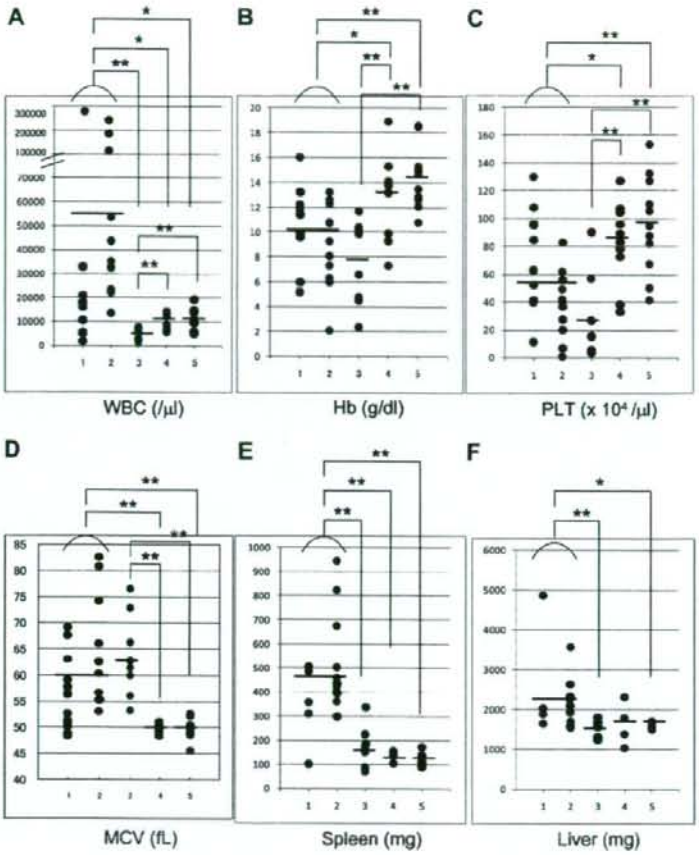

Figure 3. Peripheral white blood cell counts of mice/D171N showed leukocytosis, while mice/S291fs showed leukopenia. (A) Counts of white blood cells (WBCs) in PB. (B) Concentration of hemoglobin (Hg). (C) Counts of platelets (PLT). (D) Red cell MCV. (E,F) Weight of spleen and liver of morbid mice (mice/D171N or S291fs) or 1-year-old healthy mice (mice/WT or mock). Statistical differences were determined by 2-sample *t* test with Welch correction (*$P < .05$; **$P < .01$). Lane 1: mice/D171N without high expression of *Evi1* in BM or not examined due to the lack of bone marrow samples (WBC, PLT, Hg, and MCV: n = 11; spleen: n = 5; and liver: n = 4). Lane 2: mice/D171N with high expression of *Evi1* (n = 11). Lane 3: mice/S291fs (WBC, PLT, Hg, and MCV: n = 9; spleen and liver: n = 8). Lane 4: mice/WT (WBC, PLT, Hg, and MCV: n = 10; spleen and liver: n = 4). Lane 5: mice/mock (WBC, PLT, Hg, and MCV: n = 12; spleen: n = 6; and liver: n = 5).

and died with shorter latencies. Hematologic parameters of mice that underwent serial transplantation are shown in Table S3.

In summary, the pattern and degree of multilineage dysplasia differed among the mice that underwent transplantation. Although both mice/D171N and mice/S291fs died of MDS and MDS/AML within 4 to 13 months after transplantation, a marked difference existed in terms of clinical symptoms, including hematopoietic or macroscopic findings.

A distinct type of disease was identified in mice/D171N

Among the mice that underwent transplantation transduced with AML1-D171N, a distinct group was identified. GFP$^+$ BM cells in 11 of 16 morbid mice/D171N (mouse IDs 4, 6, 7, 12-15, 19, 20, 22, and 26) displayed a similar phenotype, with high percentages of CD11b$^+$ and B220$^+$ cells (Figure 5; data not shown). All these mice/D171N showed dysplasia in myeloid and erythroid lineages for several months and died of MDS/AML with increased number of blasts, anemia, and, in some cases, thrombocytopenia (Table S2). These mice/D171N also showed severe hepatosplenomegaly (Figures 3E,F, 6A; Table S2), and histologic examination showed expansion of blasts and immature myeloid cells in the PB, BM, and spleen, and the invasion of these cells into hepatic portal areas in the liver and spaces among renal tubules in the kidney (Figure 6B,D,F). Giemsa staining of BM showed a high percentage of blasts (Figure 6H), in accordance with a high percentage of both GFP/c-kit double-positive cells by flow cytometolic analysis.

In contrast, the remaining 4 morbid mice/D171N diagnosed as MDS (mouse IDs 9 and 11) or MDS/AML (mouse IDs 10 and 17) showed heterologous phenotypes of GFP$^+$ BM cells (data not shown). Although mouse IDs 9 and 17 displayed hepatosplenomegaly like other mice/D171N, they exhibited leukocytopenia with fewer blasts.

AML1-D171N collaborated with *Evi1* in inducing MDS/AML

We then asked why even the same point mutant of *AML1* caused different phenotypes of MDS-RAEB and MDS/AML. We assumed the possibility that the integration of retroviruses influenced the outcomes in the BMT model. To explore this, we first performed Southern blot analysis of BM of the morbid mice. A single or several proviral integrations were confirmed (Figure 7A). Next, we used the bubble PCR method to identify the integrated sites.[7,44,45] A single or 2 integration sites were identified in each sample (Table 1). Interestingly, integrations near *Evi1* site were found in 7 of 15 genomic DNA samples of BM cells derived from mice/D171N, but not from mice/S291fs. Moreover, retrospective examination revealed that these 7 mice presented nearly identical phenotypes, characterized by marked hepatosplenomegaly (Figure 6A), leukocytosis (Figure 3A), and biphenotypic surface markers (CD11b$^+$

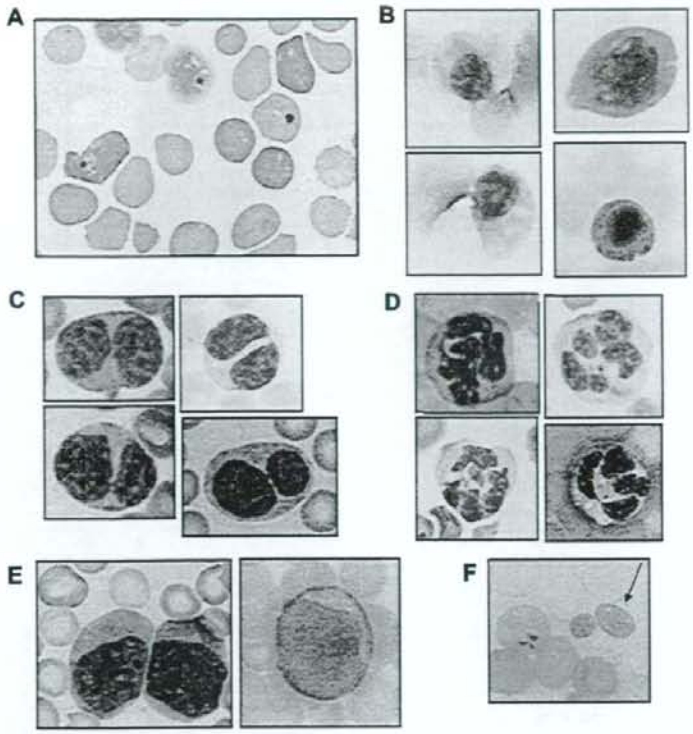

Figure 4. Multilineage dysplasia of hematopoietic cells in mice that received transplants of *AML1* mutants. Giemsa-stained PB smears obtained from mice/D171N or S291fs are shown. (A) Howell-Jolly body, polychromasia, and anisopoikilocytosis. (B) Orthochromatic giant erythroblast, karyorrhexis, and nuclear fragments. (C) Pseudo-Peiger-Huet anomaly. (D) Hypersegmented neutrophil. (E) Blasts in peripheral blood. (F) Giant platelet. Images were obtained with a BH51 microscope and DP12 camera (Olympus, Tokyo, Japan); objective lens, UPlanFI (Olympus); magnification, ×1000.

and B220$^+$) of the leukemic cells (Figure 5), thus constituting a definite subgroup among mice/D171N. Southern blot analysis showed that all of the leukemic mice with high expression of Evi1 are monoclonal (except for mouse IDs 15 and 19), but the other leukemic mice without high expression of Evi1 are oligoclonal or have several integrations (Figure 7A). Noteworthy was the finding that the *Evi1* site was not identified from the genomic DNA samples of mice/S291fs, even though the *Evi1* site is a known common integration site of retroviruses.[31-38] These led us to postulate that Evi1 collaborated with AML1-D171N in inducing the distinct type of MDS/AML. To test this, we examined whether the expression of *Evi1* was enhanced in the BM cells in which the integration into an *Evi1* site was identified. Real-time PCR analysis demonstrated that the expression levels of *Evi1* were high in all the related samples (Figure 7C). Protein expression levels corresponded to mRNA expression levels of Evi1 (Figure 7D; data not shown). Interestingly, 4 samples derived from mice/D171N harboring no integration near *Evi1* also displayed significantly high expression levels of *Evi1* (mouse IDs 13, 19, 20, and 22), and the phenotypes of these mice were identical to those induced by AML1-D171N–transduced cells in which retroviruses were integrated into the *Evi1* site. In these cases, the expression of *Evi1* might have been enhanced secondarily by an unknown mechanism, or we simply failed to detect the integration site. The latter possibility was supported by the fact that multiple integrations were detected in these cases (Figure 7A; mouse IDs 13, 19, and 20). In any case, all the mice/D171N with enhanced expression of Evi1 in their BM cells displayed high percentages of blasts (Figure S1). We also examined whether the expression of MDS1/Evi1 was enhanced by the integration into an *Evi1* site. The *MDS1* gene is located approximately 240 kb upstream of Evi1, and MDS1/Evi1 is generated from the in-frame splicing of MDS1 to the second exon of Evi1.[36,43] Real-time PCR analysis demonstrated that the expression levels of MDS1/Evi1 were low and were not significantly increased when compared with controls (data not shown). The integration sites of *Evi1* were focused on two regions (Table 1). One is 15 kb upstream of start site of *Evi1* (mouse IDs 12, 14, 15), and another is 107 kb upstream of start site of *Evi1* (mouse IDs 4, 6, 7, 26). Morishita et al reported that the retrovirus integrations had occurred near or in 5′ noncoding exons of *Evi1* gene.[31] The integration site at 15 kb upstream of the start site of *Evi1* that we found is near to the site they reported.

In vivo collaboration between *Evi1* and AML1-D171N

Next, we tested to see if *Evi1* expression collaborates with AML1-D171N in inducing leukemia in the BMT model. Cotransduction of AML1-D171N and Evi1 into BM cells resulted in rapid induction of the disease in the mice that underwent transplantation that was essentially identical with the disease that developed after a long latency in the mice/D171N (Figures 1E,5). In fact, all the mice displayed increased number of blasts in the PB within a month after the transplantation of BM cells transduced with Evi1/D171N. Southern blot analysis showed that these leukemic cells were polyclonal (Figure 7B). These results indicate that AML1-D171N and Evi1 collaborate to induce MDS/AML with a distinct phenotype. On the other hand, cotransduction of AML1-S291fs and *Evi1* into BM cells did not induce MDS/AML in 5 months (data not shown). In the present work, mice that received transplants of BM cell–transduced *Evi1* alone did not present any abnormalities in 5 months (Figure 1E).

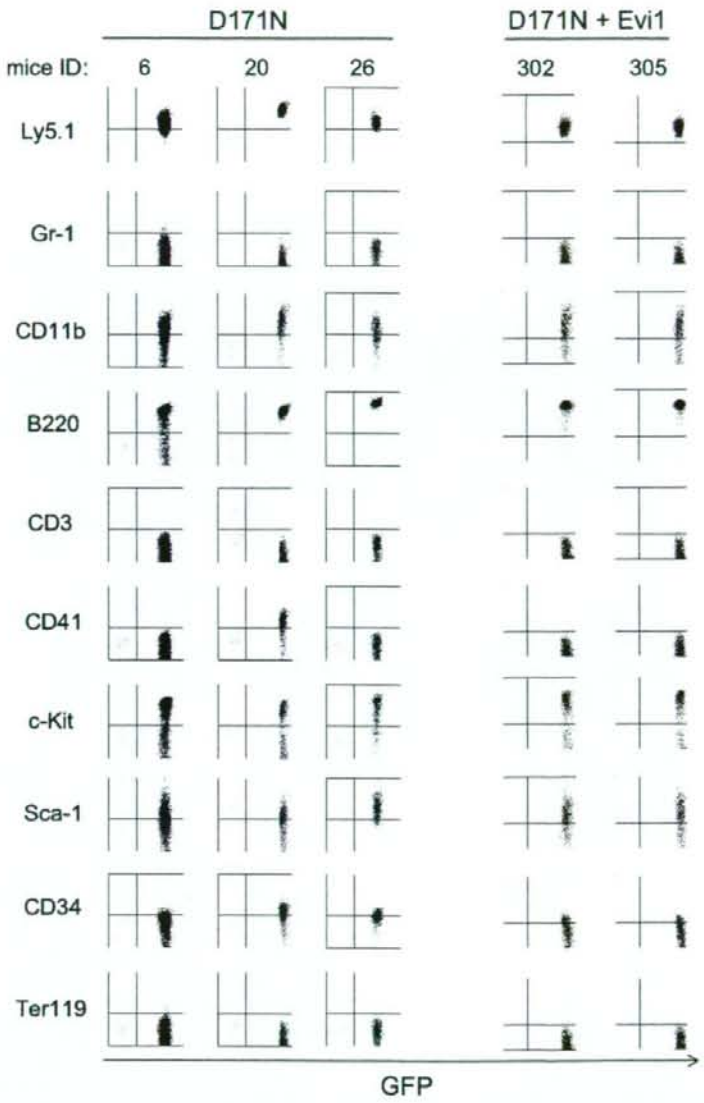

Figure 5. AML1-D171N induced a biphenotypic leukemia in concert with Evi1 in the BMT model. The dot plots show Ly5.1, Gr-1, CD11b, B220, CD3, CD41, c-kit, Sca-1, CD34, or Ter119 labeled with a corresponding PE-conjugated mAb versus expression of GFP. BM cells of morbid mice/D171N with high expression of *Evi1* (mouse IDs 6, 20, and 26) and those of morbid mice/D171N + *Evi1* (mouse IDs 302 and 305) displayed a similar pattern of surface markers, $CD11b^+$ and $B220^+$.

AML1-S291fs induced erythroid dysplasia with pancytopenia

In contrast to mice/D171N, most of mice/S291fs displayed remarkable erythroid dysplasia with continuous pancytopenia (Figures 3A-C,4A). A total of 2 of 8 mice/S291fs died of MDS-RAEB in which the percentage of blasts in the bone marrow was less than 20%, and 5 mice/S291fs developed MDS/AML. The mice displayed severe anemia but not leukocytosis in the PB, and the numbers of blasts were generally lower than those of MDS/AML mice transduced with AML1-D171N (Table S2). Surface markers of leukemic cells derived from mice/S291fs were different from those of mice/D171N (Figure S3).

We found integrations of the retrovirus in the intron of MN1 in 3 of 8 mice/S291fs (Table 1; mouse IDs 55, 56, and 58), and MN1 was overexpressed in the leukemic cells of these mice (Figure S2). The integration site was identical among these leukemic cells, indicating that leukemic cells of the 3 mice were derived from a single hematopoietic progenitor and that overexpression of MN1 induced expansion of the transduced stem cells during the 3-day culture period before the transplantation. Indeed, the mice with the integration at that MN1 site developed MDS/AML with shorter latencies (Table S2).

Discussion

We have established a mouse BMT model for MDS and MDS/AML using *AML1* mutants derived from patients with MDS,

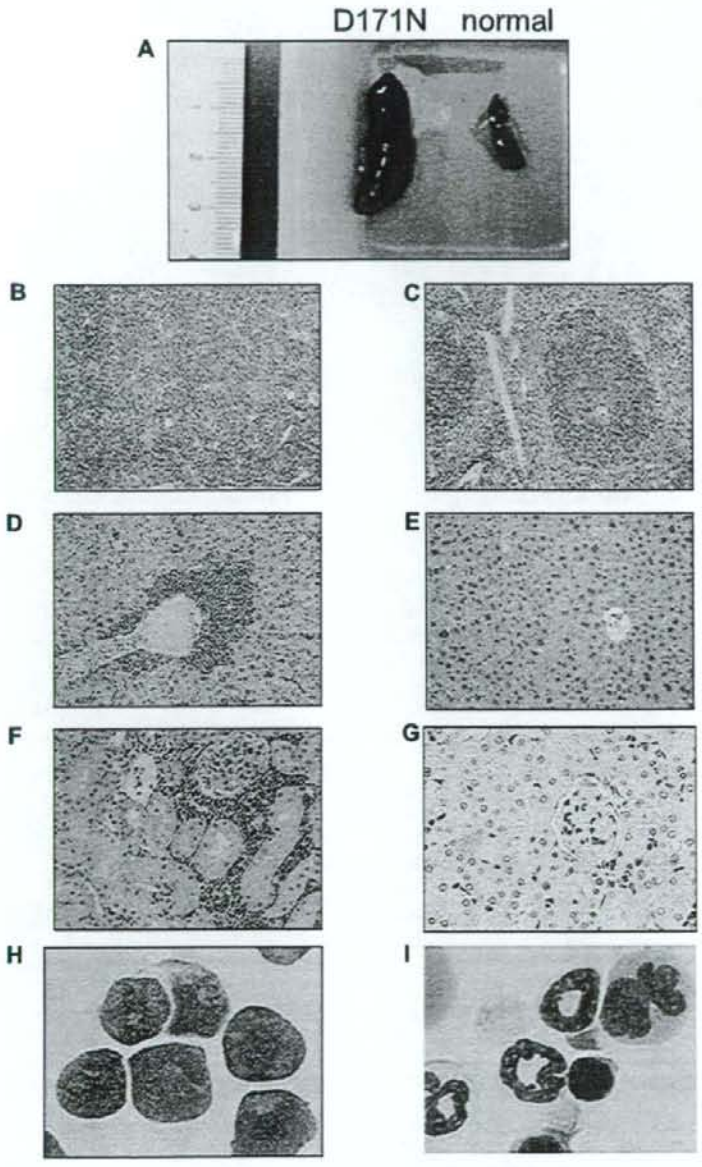

Figure 6. Leukemic cells of mice/D171N with high expression of Evi1 invaded into liver and kidney. (A) Spleen from morbid mice/D171N (left) and from normal mice (right). Histopathologic findings of (B) spleen, (D) liver, and (F) kidney infiltrated with leukemic cells from mice/D171N, stained with H&E. Histopathologic findings of (C) spleen, (E) liver, and (G) kidney from normal mice, stained with H&E. (H) Mice/D171N showed a high percentage of blasts in bone marrow. Cytospin preparations of BM cells from (H) mice/D171N and (I) normal mice, stained with Giemsa. (BX51 microscope, DP12 camera module; objective lens, UPlanFl; magnification, ×200 (B-E); ×100 (F,G); and ×1000 (H,I).

although previous studies either using similar BMT models or knock-in mice of *AML1* mutants failed to do so. There are several potential explanations for this discrepancy. First, because most *AML1* mutants work as dominant-negative forms, high expression levels of the mutants would be critical to effectively inhibit WT *AML1*. In this aspect, our BMT model has an advantage, using the efficient retrovirus vector pMYs[40] designed to achieve high expression in hematopoietic progenitor cells and, unlike most other retrovirus vectors, harbors splice donor and acceptor sites derived from the MFG vector to increase expression levels.[40,47] Second, using the efficient packaging cell line Plat-E,[39] we achieved high titers of retroviruses (average: 10^7 infection U/mL), which could result in the higher numbers of retrovirus integrations. This also increases the probabilities of up-regulating or disrupting important genes that collaborate with *AML1* mutants in inducing MDS and/or MDS/AML. Alternatively, it is also possible that the positions of *AML1* mutations are critical for the biological effect. We believe that the combination of these factors has put our system into practice.

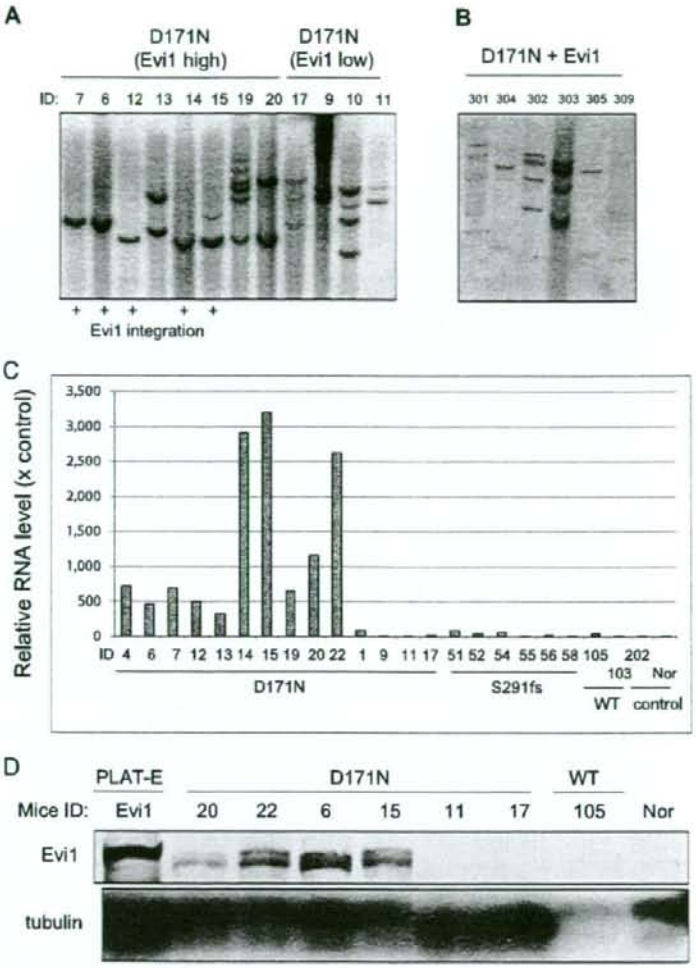

Figure 7. The mice/D171N with integration near *Evi1* site were monoclonal. (A) Southern blot analysis of mice/D171N. DNA samples were digested with *Eco*RI, which cut the retrovirus only once within the multicloning site. Probes used were DNA fragments of the GFP coding sequence. Mouse IDs are shown at the top of the panel. (B) The mice/D171N + *Evi1* were polyclonal. DNA samples were digested with *Eco*RI. Proviruses were probed with a GFP probe. (C) Real-time PCR for *Evi1* in BM derived from morbid mice/D171N or mice/S291fs or mice/WT or mice/mock. In addition to 6 samples from mice/D171N harboring integration near *Evi1* (mouse IDs 4, 6, 7, 12, 14, and 15), 4 samples derived from mice/D171N without integration near *Evi1* display high expression levels of Evi1 (mouse IDs 13, 19, 20, and 22). RNA from normal BM cells served as a control (RNA level = 1). (D) Western blot of lysates from spleen cells of mice/D171N, mice/WT, and normal mice and PLAT-E as controls. Samples from mice/D171N confirmed high expression of *Evi1* by RT-PCR showed expression of the protein (mouse IDs 6, 15, 20, and 22), but the other mice without high expression of *Evi1* by RT-PCR did not express the protein (mouse IDs 11, 17, and 105).

In the present MDS model, we used 2 *AML1* mutants, D171N and S291fsX300. The latter, a C-terminal–truncated form, is more potent as a dominant-negative form than the former, which harbors a point mutation in the RHD.[25,26] In this context, it is reasonable that the S291fs mutant induced the disease in the mice that underwent transplantation with a higher penetrance (Figure 1D). More important, expression of these mutants induced MDS/AML of distinct phenotypes in the mice that underwent transplantation: AML1-S291fs induced pancytopenia associated with dysplasia in the erythroid lineage, while AML1-D171N frequently induced hepatosplenomegaly and leukocytosis associated with marked myeloid dysplasia. This suggests that even different mutations of the same gene could induce heterogeneous diseases. As previously described,[25,26] AML1-D171N lost DNA-binding ability and hence transactivation potential because it possessed a point mutation in RHD essential for DNA-binding, while AML1-S291fs had increased DNA-binding ability but lost transactivation potential because it had an intact RHD but lacked a C-terminal transactivation domain. Thus, the different biological outcomes induced by *AML1* mutants could be explained in part by structural and functional differences between the mutants. In addition to the dominant-negative functions, these mutants may also have gain of function; the fact that AML1-KO mice did not develop leukemia[18] indicates that deletion of *AML1* alone is not sufficient to induce leukemia, suggesting the possibility that the *AML1* mutants have gain of function as well. Because *AML1* associates and forms a ternary complex with other transcriptional factors and cofactors via its specific domains, it is possible that these mutants exert different effects on the proliferation and differentiation of BM cells in the various contexts.

In BMT models using retrovirus-mediated gene transfer, the genes near the retrovirus integration sites are thought to affect the outcomes.[30-38] This sometimes obscures the significance of the transduced gene, but simultaneously will give us clues to understanding the collaboration of multiple genes in the development of leukemias. One of the intriguing findings of the present work is that high expression of *Evi1*, either caused by virus integration or by unknown mechanisms, was able to collaborate with AML1-D171N in inducing the homogeneous disease characterized by leukocytosis, severe myelodysplasia, and marked hepatosplenomegaly that

Table 1. Analysis of integration site

Mutant	Mouse ID	Count of Southern blot bands	Nearest gene	Chromosome no.	Gene ID	Distance to gene (start or end), bp	Location	Forward or reverse orientation	RTCGD hits
Experiment 1									
D171N	1	ND	*2010111I01Rik*	13	72061	238 927	Intron 10	F	0
D171N	1		*LOC100040862*	12	100040862	40 051	5′	F	0
D171N	4	ND	*Evi1*	3	14013	107 412	5′	R	24
D171N	4		*Nsmce2*	15	68501	221 183	Intron 5	R	2
Experiment 2									
D171N	5	3	*Rreb1*	13	68750	14 071	5′	R	9
D171N	5		*LOC619665*	6	619665	123 854	5′	F	0
D171N	6	1	*Evi1*	3	14013	106 286	5′	R	24
D171N	7	1	*Evi1*	3	14013	106 286	5′	R	24
Experiment 3									
D171N	10	4	*B4galt6*	18	56386	8 961	Intron 1	R	0
D171N	11	2	*Rp1h*	1	19888	65 523	5′	F	0
Experiment 4									
D171N	12	1	*Evi1*	3	14013	14 909	5′	F	24
D171N	13	2	*Slc38a2*	15	67760	41 018	5′	F	6
D171N	14	1	*Evi1*	3	14013	15 002	5′	F	24
D171N	15	2	*Evi1*	3	14013	14 850	5′	F	24
D171N	15		*Slc38a2*	15	22462	11 988	5′	R	6
S291fsX300	51	ND	*LOC100042800*	13	100042800	27 734	5′	R	0
S291fsX300	52	2	*P2rx7*	5	18439	40 672	intron 13	R	1
S291fsX300	52		*Gm pr2*	14	105446	17	intron 1	R	0
S291fsX300	54	2	*M srb3*	10	320183	98 981	3′	F	0
Empty	203	ND	*Dph5*	3	13609	70 064	5′	R	1
Experiment 5									
D171N	19	6	*Gch1*	14	14528	16 958	Intron 1	R	0
D171N	20	2	*Gch1*	14	14528	16 958	Intron 1	R	0
S291fsX300	55	2	*Mn1*	5	433938	16 024	Intron 1	F	8
S291fsX300	56	1	*Mn1*	5	433938	16 024	Intron 1	F	8
S291fsX300	58	1	*Mn1*	5	433938	16 024	Intron 1	F	8
Experiment 6									
D171N	22	ND	*Lrrc8c*	5	100604	16 056	5′	F	4
Experiment 7									
D171N	26	1	*Evi1*	3	14013	106 710	5′	F	24
S291fsX300	60	3	*Dock10*	1	210293	163 158	Intron 1	R	0

RTGCD, Retroviral Tagged Cancer Gene Database[37]; and ND, not determined.

always developed to overt leukemia with high percentages of B220$^+$ and CD11b$^+$ blasts. Together with the recent findings that Evi1 expression was observed in patients with MDS and AML,[36,48] and that Evi1 alone did not induce AML in mouse models,[14,34,49,50] our result strongly suggested that AML1-D171N collaborated with Evi1 in inducing MDS/AML. It is interesting to note that AML1-S291fs never collaborated with *Evi1* during our examination (Table 1), again suggesting that these 2 *AML1* mutations transform hematopoietic cells through distinct mechanisms. Importantly, we confirmed the collaboration between AML1-D171N and *Evi1* in an in vivo experiment. Cotransduction of AML1-D171N and *Evi1* into BM cells resulted in rapid induction of MDS/AML in the mice that received transplants. In addition, the leukemic cells in most of these mice included more clones than those in mice/D171N (Figure 7B), indicating cooperation of *Evi1* and AML1-D171N. However, leukemic cells from one mouse (ID 305) seemed to be monoclonal and to contribute to oligoclonal leukemia of mouse 304. In addition, it took 2 to 3 months for leukemias induced by the combination of AML1-D171N and Evi1 to kill the mice that received transplants. Together, these result suggested that while AML1-D171N and Evi1 overexpression collaborated in inducing leukemia, additional steps were required for efficient transformation of hematopoietic progenitors. In the absence of Evi1 high expression, AML1-D171N caused MDS or MDS/AML with low percentages of blasts in BM but still with hepatosplenomegaly. This indicates that hepatosplenomegaly had something to do with AML1-D171N.

In contrast to mice/D171N, most mice/S291fs succumbed to either MDS-RAEB with fatal severe anemia following continuous pancytopenia or MDS/AML without leukocytosis. The integration site in the intron 1 of the *MN1* gene found in leukemic cells of 3 mice was derived from the same cell. We also found that *MN1* was overexpressed in the leukemic cells of these mice, suggesting that overexpression of *MN1* induced effective expansion of leukemic stem cells. Recently, Heuser et al reported that high expression of *MN1* correlated with poor outcome in AML with normal cytogenetics.[51] Moreover, Slape et al identified *MN1* as potential collaborators of NUP98/HOXD13 to induce leukemia.[42] Further work will be required to investigate the role of MN1 in MDS/AML.

One fundamental question of this study was whether *AML1* mutants alone induce MDS and MDS/AML. In our experiments, 5 of the 6 surviving mice/D171N showed a disappearance of GFP$^+$ cells in time, suggesting that AML1-D171N alone was not able to induce MDS/AML. Previous studies using gene-engineered mice and a BMT model demonstrated that *AML1*

fusions caused by chromosomal translocations alone were insufficient to induce AML,[7-12] except for *AML1-MDS1-Evi1*, which by itself induced AML with a long latency.[52] In addition, several lines of evidence[30-38] that implicated the integration site of retroviruses for different biological outcomes led us to consider the same possibility in this BMT model. Indeed, we identified frequent retrovirus integrations near the *Evi1* gene in the BM cells derived from mice/D171N whose leukemic cells displayed nearly identical phenotypes and concomitant elevated expression of *Evi1*. Importantly, coexpression of AML1-D171N and *Evi1* induced the same leukemia with shorther latencies, demonstrating the collaboration between AML1-D171N and *Evi1* in vivo. These results showed the power of in vivo insertional mutagenesis of retroviruses in a search for genes involved in the pathogenesis of MDS and MDS/AML.

Finally, it is important to relate these in vivo results to clinical data of the human disease. The recent finding[25-27] that *AML1* point mutations in the C-terminal regions were almost exclusively found in MDS-RAEB and MDS/AML, but not in de novo AML, coincided with our data that AML1-S291fs tended to induce MDS-RAEB–like symptoms in this BMT model. Clinical findings[25-27] that the RHD point mutation was often found in de novo AML, mainly AML M0, in addition to MDS-RAEB and MDS/AML, was also in accordance with our data that AML1-D171N induced more progressive MDS/AML with higher percentages of blasts when compared with AML1-S291fs. Classification of MDS and MDS/AML is always controversial because of the heterogeneity of the disease.[1,2,27] In the future, this disease will be reclassified based on genetic alterations and their combinations.

In summary, we have generated a mouse BMT model of MDS-RAEB and MDS/AML. The current BMT model, mimicking AML1-related MDS, will be useful for understanding molecular pathogenesis and establishing new therapeutic strategy for MDS and MDS/AML.

Acknowledgments

We greatly thank Dr Mineo Kurokawa for kindly providing the anti-*Evi1* antibody and Dr Takuro Nakamura and Dr Kazuhiro Morishita for kindly providing pMYs-*Evi1*-IG. We also thank Dr Christopher Slape for kindly giving information about the condition of RT-PCR for MN1. We are grateful to Dr Dovie Wylie for excellent language assistance. We thank Yumi Fukuchi, Fumi Shibata, Miyuki Ito, and Ai Hishiya for technical assistance.

This work was supported by the Grant-in-aid for Cancer Research supported by the Ministry of Health, Labor and Welfare, Japan; a grant from the Vehicle Racing Commemorative Foundation; and a grant from the Japan Society for the Promotion of Science (JSPS). N.W.-O. is a JSPS research fellow.

Authorship

Contributions: N.W.O. did all the experiments and participated in writing the manuscript; J.K. oversaw all the experiments and actively participated in manuscript writing; R.O. provided experimental guidance about and assisted in the BMT model; H.H. provided the general information and made the constructs of AML1 mutants; Y.H. made the constructs of AML1 mutants; Y.K. assisted in the experiments of BMT model; H.N. provided experimental guidance about cell sorting and staining; T.N. provided experimental guidance of the BMT model; T.I. provided the general information and constructs of AML1 mutants; and T.K. conceived and directed the project, secured funding, and actively participated in manuscript writing.

Conflict-of-interest disclosure: The authors declare no competing financial interests.

Correspondence: Toshio Kitamura, Division of Cellular Therapy, Advanced Clinical Research Center, The Institute of Medical Science, The University of Tokyo, 4-6-1 Shirokanedai, Minato-ku, Tokyo 108-8639, Japan; e-mail: kitamura@ims.u-tokyo.ac.jp.

References

1. Mufti G, List AF, Gore SD, Ho AY. Myelodysplastic syndrome. Am Soc Hematol Educ Program. 2003;176-199.
2. Heaney ML, Golde DW. Myelodysplasia. N Engl J Med. 1999;340:1649-1660.
3. Legare RD, Gilliland DG. Myelodysplastic syndrome. Curr Opin Hematol. 1995;2:283-292.
4. Hirai H, Kobayashi Y, Mano H, et al. A point mutation at codon 13 of the N-ras oncogene in myelodysplastic syndrome. Nature. 1987;327:430-432.
5. Hirai H, Okada M, Mizoguchi H, et al. Relationship between an activated N-ras oncogene and chromosomal abnormality during leukemic progression myelodysplastic syndrome. Blood. 1988; 71:256-258.
6. Gilliland DG, Griffin JD. Role of FLT3 in leukemia. Curr Opin Hematol. 2002;9:274-281.
7. Schessl C, Rawat VP, Cusan M, et al. The AML1-ETO fusion gene and the FLT3 length mutation collaborate in inducing acute leukemia in mice. J Clin Invest. 2005;115:2159-2168.
8. Okuda T, Cai Z, Yang S, et al. Expression of a knocked-in AML1-ETO leukemia gene inhibits the establishment of normal definitive hematopoiesis and directly generates dysplastic hematopoietic progenitors. Blood. 1998;91:3134-3143.
9. Rhoades KL, Hetherington CJ, Harakawa N, et al. Analysis of the role of AML1-ETO in leukemogenesis, using an inducible transgenic mouse model. Blood. 2000;96:2108-2115.
10. Higuchi M, O'Brien D, Kumaravelu P, Lenny N, Yeoh EJ, Downing JR. Expression of a conditional AML1-ETO oncogene bypasses embryonic lethality and establishes a murine model of human t(8;21) acute myeloid leukemia. Cancer Cell. 2002;1:63-74.
11. Fenske TS, Pengue G, Mathews V, et al. Stem cell expression of the AML1/ETO fusion protein induces a myeloproliferative disorder in mice. Proc Natl Acad Sci U S A. 2004;101:15184-15189.
12. de Guzman CG, Warren AJ, Zhang Z, et al. Hematopoietic stem cell expansion and distinct myeloid developmental abnormalities in a murine model of the AML1-ETO translocation. Mol Cell Biol. 2002;22:5506-5517.
13. Ono R, Nakajima H, Ozaki K, et al. Dimerization of MLL fusion proteins and FLT3 activation synergize to induce multiple-lineage leukemogenesis. J Clin Invest. 2005;115:919-929.
14. Buonamici S, Li D, Chi Y, et al. EVI1 induces myelodysplastic syndrome in mice. J Clin Invest. 2004;114:713-719.
15. Lin YW, Slape C, Zhang Z, Aplan PD. NUP98-HOXD13 transgenic mice develop a highly penetrant, severe myelodysplastic syndrome that progresses to acute leukemia. Blood. 2005;106: 287-295.
16. Okuda T, van Deursen J, Hiebert SW, Grosveld G, Downing JR. AML1, the target of multiple chromosomal translocations in human leukemia, is essential for normal fetal liver hematopoiesis. Cell. 1996;84:321-330.
17. Wang Q, Stacy T, Binder M, et al. Disruption of the Cbfa2 gene causes necrosis and hematorrhaging in the central nervous system and blocks definitive hematopoiesis. Proc Natl Acad Sci U S A. 1996;93:3444-3449.
18. Ichikawa M, Asai T, Saito T, et al. AML-1 is required for megakaryocytic maturation and lymphocytic differentiation, but not for maintenance of hematopoietic stem cells in adult hematopoiesis. Nat Med. 2004;10:299-304.
19. Song WJ, Sullivan MG, Legare RD, et al. Haploinsufficiency of CBFA2 causes familial thrombocytopenia with propensity to develop acute myelogenous leukaemia. Nat Genet. 1999;23:166-175.
20. Michaud J, Wu F, Osato M, et al. In vitro analyses of known and novel RUNX1/AML1 mutations in dominant familial platelet disorder with predisposition to acute myelogenous leukemia: implications for mechanisms of pathogenesis. Blood. 2002;99:1364-1372.
21. Osato M, Asou N, Abdalla E, et al. Biallelic and heterozygous point mutations in the runt domain of the AML1/PEBP2alphaB gene associated with myeloblastic leukemias. Blood. 1999;93:1817-1824.
22. Preudhomme C, Warot-Loze D, Roumier C, et al. High incidence of biallelic point mutations in the Runt domain of the AML1/PEBP2alpha B gene in

Mo acute myeloid leukemia and in myeloid malignancies with acquired trisomy 21. Blood. 2000; 96:2862-2869.

23. Imai Y, Kurokawa M, Izutsu K, et al. Mutations of the AML1 gene in myelodysplastic syndrome and their functional implications in leukemogenesis. Blood. 2000;96:3154-3160.
24. Langabeer SE, Gale RE, Rollinson SJ, Morgan GJ, Linch DC. Mutations of the AML1 gene in acute myeloid leukemia of FAB types M0 and M7. Genes Chromosomes Cancer. 2002;34:24-32.
25. Harada H, Harada Y, Tanaka H, Kimura A, Inaba T. Implications of somatic mutations in the AML1 gene in radiation-associated and therapy-related myelodysplastic syndrome/acute myeloid leukemia. Blood. 2003;101:673-680.
26. Harada H, Harada Y, Niimi H, Kyo T, Kimura A, Inaba T. High incidence of somatic mutations in the AML1/RUNX1 gene in myelodysplastic syndrome and low blast percentage myeloid leukemia with myelodysplasia. Blood. 2004;103:2316-2324.
27. Osato M. Point mutations in the RUNX1/AML1 gene: another actor in RUNX leukemia. Oncogene. 2004;23:4284-4296.
28. Steensma DP, Gibbons RJ, Mesa RA, Tefferi A, Higgs DR. Somatic point mutations in RUNX1/CBFA2/AML1 are common in high-risk myelodysplastic syndrome, but not in myelofibrosis with myeloid metaplasia. Eur J Haematol. 2005;74:47-53.
29. Christiansen DH, Andersen MK, Pedersen-Bjergaard J. Mutations of AML1 are common in therapy-related myelodysplasia following therapy with alkylating agents and are significantly associated with deletion or loss of chromosome arm 7q and with subsequent leukemic transformation. Blood. 2004;104:1474-1481.
30. Yamashita N, Osato M, Huang L, et al. Haploinsufficiency of Runx1/AML1 promotes myeloid features and leukaemogenesis in BXH2 mice. Br J Haematol. 2005;131:495-507.
31. Morishita K, Parker DS, Mucenski ML, Jenkins NA, Copeland NG, Ihle JN. Retroviral activation of a novel gene encoding a zinc finger protein in IL-3-dependent myeloid leukemia cell lines. Cell. 1988;54:831-840.
32. Mucenski ML, Taylor BA, Ihle JN, et al. Identification of a common ecotropic viral integration site, Evi1, in the DNA of AKXD murine myeloid tumors. Mol Cell Biol. 1988;8:301-308.
33. Calmels B, Ferguson C, Laukkanen MO, et al. Recurrent retroviral vector integration at the Mds1/Evi1 locus in nonhuman primate hematopoietic cells. Blood. 2005;106:2530-2533.
34. Kustikova O, Fehse B, Modlich U, et al. Clonal dominance of hematopoietic stem cells triggered by retroviral gene marking. Science. 2005;308: 1171-1174.
35. Modlich U, Kustikkova OS, Schmidt M, et al. Leukemias following retroviral transfer of multidrug resistance 1 (MDR1) are driven by combinatorial insertional mutagenesis. Blood 2005;105:4235-4246.
36. Nucifora G, Laricchia-Robbio L, Senyuk V. Evi1 and hematopoietic disorders: history and perspectives. Gene. 2006;368:1-11.
37. Akagi K, Suzuki T, Stephens RM, Jenkins NA, Copeland NG. RTCGD: retroviral tagged cancer gene database. Nucleic Acids Res. 2004;32:523-527.
38. Jin G, Yamazaki Y, Takuwa M, et al. Trib1 and Evi1 cooperate with Hoxa and Meis1 in myeloid leukemogenesis. Blood. 2007;109:3998-4005.
39. Morita S, Kojima T, Kitamura T. Plat-E: an efficient and stable system for transient packaging of retroviruses. Gene Ther. 2000;7:1063-1066.
40. Kitamura T, Koshino Y, Shibata F, et al. 2003. Retrovirus-mediated gene transfer and expression cloning: powerful tools in functional genomics. Exp. Hematol. 2003;31:1007-1014.
41. Kogan SC, Ward JM, Anver MR, et al. Bethesda proposals for classification of nonlymphoid hematopoietic neoplasms in mice. Blood. 2002;100: 238-245.
42. Slape C, Hartung H, Lin YW, et al. Retroviral insertional mutagenesis identifies genes that collaborate with NUP98-HOXD13 during leukemic transformation. Cancer Res. 2007;67:5148-55.
43. Wimmer K, Vinatzer U, Zwirn P, et al. Comparative expression analysis of the antagonistic transcription factors EVI1 and MDS1-EVI1 in murine tissues and during in vitro hematopoietic differentiation. Biochem Biophys Res Commun. 1998; 252:691-6.
44. Riley J, Butler R, Ogilvie D, et al. A novel, rapid method for the isolation of terminal sequences from yeast artificial chromosome (YAC) clones. Nucl. Acids Res. 1990;18:2887-2890.
45. Arnold C, Hodgson IJ. Vectorette PCR: a novel approach to genome walking. PCR Methods Appl. 1991;1:39-42.
46. Tsuzuki S, Hong D, Gupta R, Matsuo K, Seto M, Enver T. Isoform-specific potentiation of stem and progenitor cell engraftment by AML1/RUNX1. PLoS Med. 2007;4:e172.
47. Riviere I, Brose K, Mulligan RC. Effects of retroviral vector design on expression of human adenosine deaminase in murine bone marrow transplant recipients engrafted with genetically modified cells. Proc Natl Acad Sci U S A. 1995; 92:6733-6737.
48. Langabeer SE, Rogers JR, Harrison G, et al. EVI1 expression in acute myeloid leukaemia. Br J Haematol. 2001;112:208-211.
49. Cuenco GM, Ren R. Both AML1 and EVI1 oncogenic components are required for the cooperation of AML1/MDS1/EVI1 with BCR/ABL in the induction of acute myelogenous leukemia in mice. Oncogene. 2004;23:569-579.
50. Louz D, van den Broek M, Verbakel S, et al. Erythroid defects and increased retrovirally-induced tumor formation in Evi1 transgenic mice. Leukemia. 2000;14:1876-1884.
51. Heuser M, Beutel G, Krauter J, et al. High meningioma 1 (MN1) expression as a predictor for poor outcome in acute myeloid leukemia with normal cytogenetics. Blood. 2006;108:3898-905.
52. Cuenco GM, Nucifora G, Ren R. Human AML1/MDS1/EVI1 fusion protein induces an acute myelogenous leukemia (AML) in mice: a model for human AML. Proc Natl Acad Sci USA. 2000;97: 1760-1765.

Int J Hematol (2008) 88:82–87
DOI 10.1007/s12185-008-0103-6

ORIGINAL ARTICLE

JAK2 V617F mutation is rare in idiopathic erythrocytosis: a difference from polycythemia vera

Kentaro Yoshinaga · Naoki Mori · Yan-hua Wang · Kaori Tomita · Masayuki Shiseki · Toshiko Motoji

Received: 17 March 2008 / Accepted: 26 March 2008 / Published online: 6 June 2008

Abstract A single mutation 1849G>T in the *JAK2* gene (V617F) has recently been described in classical myeloproliferative disorders (MPD). To investigate the incidence and clinical significance of the *JAK2* mutation, we performed allele-specific polymerase chain reaction (PCR) and enzyme-based assessment in 11 idiopathic erythrocytosis (IE) and 15 polycythemia vera (PV) patients. Aberrant bands indicating the V617F mutation were detected in only one of 11 patients with IE, whereas all of the 15 patients with PV showed the *JAK2* mutation. Sequence analysis was subsequently performed in the IE patient showing aberrant bands on allele-specific PCR, and a nucleotide change corresponding to the V617F mutation was detected in four of 29 clones tested. This patient might have progressed to PV according to the new WHO diagnostic criteria proposed in 2007, since a gradual increase in platelet counts was observed 4 years after the time of diagnosis. A further longitudinal study monitoring V617F positive-cells will clarify the process of progression from IE to PV in such a patient.

Keywords JAK2 · Idiopathic erythrocytosis · Polycythemia vera

K. Yoshinaga · N. Mori (✉) · Y. Wang · K. Tomita · M. Shiseki · T. Motoji
Department of Hematology,
Tokyo Women's Medical University,
8-1 Kawada-cho, Shinjuku-ku, Tokyo 162-8666, Japan
e-mail: mori@dh.twmu.ac.jp

1 Introduction

Janus kinase 2 (JAK2) is a tyrosine kinase involved in the cytokine signaling of several growth factors such as erythropoietin and thrombopoietin in normal and neoplastic cells [1]. A single mutation 1849G>T in the *JAK2* gene, which causes the substitution of phenylalanine for valine at position 617 (V617F), has recently been described in classical myeloproliferative disorders (MPD) [2–5]. The *JAK2* mutation has been found in 65–97% of patients with polycythemia vera (PV), and in half of those with essential thrombocythemia (ET) and idiopathic myelofibrosis (IMF). The *JAK2* V617F mutation was located in the pseudokinase domain, which negatively regulates activity of the kinase domain. This mutation causes the constitutive activation of the JAK2 kinase, resulting in the acceleration of cellular proliferation. Detection of the *JAK2* mutation has recently been included in the World Health Organization (WHO) diagnostic criteria for PV [6].

Idiopathic erythrocytosis (IE) is characterized by an increase in red cell mass without an identified cause [7–9]. IE differs from PV by the absence of splenomegaly, granulocytosis, and thrombocytosis. The term "pure erythrocytosis" is considered identical to IE. Najean et al. [10] reported that 10% of 51 patients diagnosed as having pure erythrocytosis at initial presentation, showed progression to PV at the late stage of the clinical course. In addition, Michiels et al. [11] proposed that IE was the first stage of PV. However, the significance of the *JAK2* V617F mutation in patients with IE remains unclear.

To investigate the incidence and clinical significance of the *JAK2* mutation in Japanese patients with IE, we performed allele-specific polymerase chain reaction (PCR) and restriction enzyme-based assessment. We also

analyzed the *JAK2* mutation in PV to elucidate the difference between IE and PV.

2 Materials and methods

2.1 Patients and samples

Peripheral blood or bone marrow samples were obtained from 11 patients with IE and 15 patients with PV. All samples were obtained under written informed consent. Diagnoses of PV were based on the criteria of the Polycythemia Vera Study Group (PVSG) or WHO 2001 [11–13]. IE was diagnosed in patients demonstrating an increased red cell mass without a known cause of secondary polycythemia and various congenital primary erythrocytosis [7–9]. Although, all 11 patients with IE showed a red cell mass over 36 mL/kg in males or 32 mL/kg in females using ^{51}Cr radioisotope, these patients did not fulfill with PV criteria due to the absence of leukocytosis and thrombocytosis at diagnosis. Splenomegaly was absent in all IE patients except one. One patient (IE No. 11) had a slight splenomegaly. The leukemic cell line HEL was used as a positive control and HL-60 was used as a negative control for the *JAK2* V617F mutation.

Neutrophils were purified by dextran sedimentation followed by hypotonic lysis and centrifugation with Ficoll-Conrey (specific gravity 1.077) as previously described by Woodman et al. [14]. Genomic DNA was extracted from neutrophils or leukemic cells using QIAamp DNA blood mini kit (Qiagen, Valencia, CA). In six IE patients, genomic DNA was extracted from smear samples of bone marrow using QIAamp DNA blood micro kit (Qiagen, Valencia, CA).

2.2 Allele-specific PCR analysis of the *JAK2* gene

Allele-specific PCR was performed using primers ALLS-JAK2-R (5′-CTGAATAGTCCTACAGTGTTTTCAGTTTCA-3′), ALLS-JAK2-F (specific) (5′-AGCATTTGGTTTTAAATTATGGAGTATATT-3′), and ALLS-JAK2-IF (internal control) (5′-ATCTATAGTCATGCTGAAAGTAGGAGAAAG-3′) as previously described by Baxter et al. [2]. The ALLS-JAK2-F primer is specific for the mutant allele and contains an intentional mismatch at the third nucleotide from the 3′ end to improve specificity. Each 20 μL of PCR reaction contained 5 μg of DNA template, 2 μL of 10× Buffer, 0.5 U of Taq polymerase (Takara, Ohtsu, Japan), dNTPs and 0.5 μL of each primer. The PCR cycling parameters were the following: one cycle of 94°C for 5 min, 36 cycles of 94°C for 60 s, 58°C for 60 s and 72°C for 60 s; followed by one cycle of 72°C for 5 min. PCR products were analyzed on a 3% agarose gel.

2.3 Restriction enzyme-based assessment of the *JAK2* gene

Amplification and sequencing of exon 14 of the *JAK2* gene was performed as previously described by Baxter et al. [2] using primers JAK2-14F (5′-GGGTTTCCTCAGAACGTTGA-3′) and JAK2-14R (5′-TCATTGCTTTCCTTTTTCACAA-3′). The PCR cycling parameters were the following: one cycle of 94°C for 5 min, 45 cycles of 94°C for 60 s, 57°C for 60 s and 72°C for 60 s; followed by one cycle of 72°C for 5 min. PCR products were purified with QIAquick PCR purification Kit (Qiagen Valencia, CA). After purification, 460-bp PCR products were digested with *Bsa*XI (New England Biolabs, Hitchin, UK) for 4 h at 37°C, and then analyzed on a 2% agarose gel.

2.4 Sequencing of the *JAK2* gene

Besides PCR products covering exon 14, exon 12 was also amplified using primers by Scott et al. [15]. Sequencing was performed in both directions using a MegaBase sequence system (Amersham, Buckingham, UK). PCR products were purified using QIAquick PCR purification Kit and subsequently analyzed by direct sequencing. In some cases, PCR products were also ligated into pGEM-T vector (Promega, Madison, WI). As a template, one of the plasmid clones containing appropriate PCR products was used for the sequencing reaction. In each case, at least three of the plasmid clones were sequenced. When an alteration in sequence was detected, additional clones were subsequently sequenced.

3 Results

Table 1 shows the clinical and laboratory data of the patients diagnosed as IE and PV. Mean patient age was younger in the IE group than in the PV group ($P = 0.01$). There was a greater male predominance in the IE group than in the PV group. MCV in the IE group was significantly larger than that of the PV group ($P = 0.01$), but there was no significant difference in hematocrit between the IE and PV groups. Red cell mass volume was similar between the IE and PV groups. Serum erythropoietin was significantly higher in the IE group than in the PV group ($P = 0.01$). Although all the patients with PV demonstrated splenomegaly, that finding was observed in only one patient with IE (IE No. 11). Bone marrow showed normocellularity in the majority of IE patients, whereas it was hypercellular in PV.

Table 2 shows the clinical and laboratory data of IE patients. Red cell mass volume was increased without a known cause of secondary polycythemia, and leukocyte

Table 1 Clinical and laboratory data at the time of diagnosis

	IE (n = 11)	PV (n = 15)	P value
Age	47 (25–59)	60 (36–70)	0.01
Male:Female	10:1	8:7	
WBC (/μL)	6,100 (4,090–7,500)	11,400 (7,000–19,400)	<0.01
RBC counts ($\times 10^6$/μL)	604 (559–730)	669 (484–812)	0.08
Hb (g/dL)	19.3 (18.5–21.4)	19.2 (18.8–22.3)	0.12
Hematocrit (%)	57.8 (52.6–65.8)	59.7 (47.7–72.5)	0.94
MCV (fL)	96.3 (85.5–100.7)	87.5 (71.4–98.6)	0.01
Platelet counts ($\times 10^4$/μL)	20.2 (14.4–34.0)	49.6 (30.7–90.6)	<0.01
Red cell mass (mL/kg)	42.9 (37.8–56.0)	44.4 (31.9–65.4)	0.39
Serum erythropoietin (mIU/L) (normal range 7.4–35 mIU/mL)	15.6 (8.5–25.7)	9.3 (3.5–13.5)	0.01
Splenomegaly	–[a]	+++	
Bone marrow cellulality	Normocellular[b]	Hypercellular	

Data are presented as the median (range)

[a] Slight splenomegaly was observed in one patient (IE No.11)

[b] One patient showed hypercellular bone marrow (IE No.11)

Table 2 Clinical and laboratory data at the time of the patients were diagnosed as having idiopathic erythrocytosis

Patient No.	Age	Sex	WBC (μL)	Neutro (%)	RBC ($\times 10^4$/μL)	Hct (%)	Plt ($\times 10^4$/μL)	RBC mass (mL/kg)	sEPO (pg/mL)	Splenomegaly	Duration from diagnosis (years)	BM cellularity	JAK2 mutation	
													PB[a]	BM
1	54	M	6,880	52.7	600	57.8	34.0	43.5	10.1	–	6.6	NE	+	NE
2	58	M	5,500	59.1	568	56.2	16.7	39.1	16.9	–	13.3	NE	–	NE
3	30	M	6,500	48.5	604	54.0	26.6	40.0	15.9	–	3.3	NE	–	NE
4	55	M	6,410	55.8	604	60.3	14.4	56.0	13.6	–	6.3	NE	–	NE
5	39	M	5,260	70.4	730	65.8	17.9	44.1	15.6	–	3.6	Normo	–	–
6	51	M	7,500	71.6	559	56.3	20.0	41.4	18.5	–	12.8	Normo	–	–[a]
7	39	M	5,610	59.6	613	60.2	24.1	42.9	17.5	–	4.0	Normo	–	–
8	36	M	6,000	49.0	566	55.3	17.8	43.2	11.4	–	17.6	Normo	–	–
9	25	M	5,430	70.4	615	52.6	23.2	37.8	13.1	–	2.7	NE	–	NE
10	59	F	4,090	39.1	698	65.2	21.5	47.1	25.7	–	8.2	Normo	–	–
11	47	M	7,400	50.0	645	60.4	20.2	38.6	8.5	+	13.6	Hyper	–	–

Neutro neutrophils, *sEPO* serum erythropoietin, *PB* peripheral blood, *BM* bone marrow, *Normo* normocellular, *Hyper* hypercellular, *NE* not examined

[a] The *JAK2* mutation was analyzed after diagnosis

counts and platelet counts were not increased in any of the patients. The duration of follow-up after diagnosis ranged from 2.7 to 17.6 years (median 6.6 years). Frequent periodic phlebotomy was required in all of the 11 patients. The clinical course and hematological data of four representative patients with IE (IE No. 1, 6, 7, and 10) are shown in Fig. 1. Leukocyte and platelet counts remained stable during observation period in all patients except one (IE No. 1). This patient had slightly higher platelet counts than the others at the time of diagnosis, and his platelet counts gradually increased to over 40 × 10^4/μL during observation (Fig. 1a).

We first performed allele-specific PCR of the *JAK2* gene with peripheral neutrophil DNA in the 11 IE and 15 PV. In Fig. 2a, the 203-bp products indicated amplified mutant allele, and the 364-bp products showed an internal control. Aberrant bands were detected in only one of the 11 IE patients (IE No.1). However, the *JAK2* V617F mutation was detected in all PV patients (data not shown). Subsequently, we performed restriction enzyme-based assessment of the

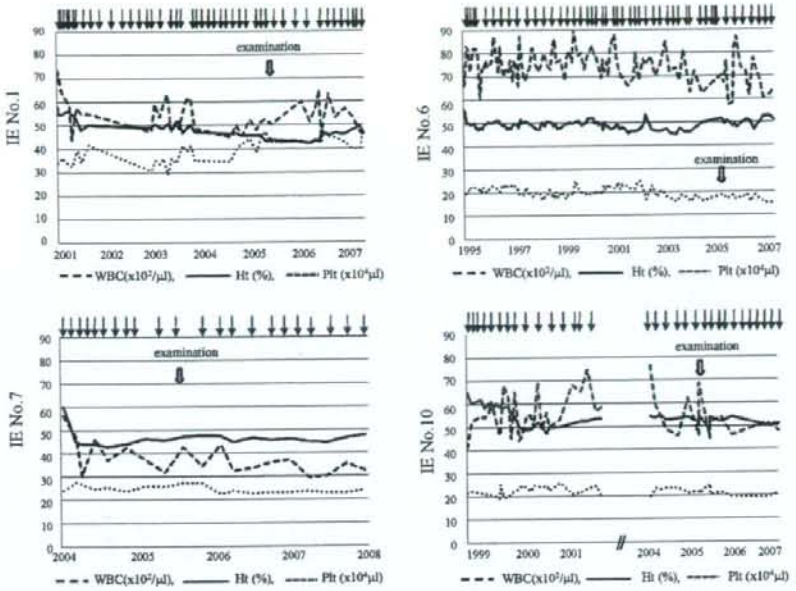

Fig. 1 Clinical course of IE patients. Clinical course and hematological data of four representative patients with IE (IE No. 1, 6, 7 and 10) are shown. *Arrow* indicates phlebotomy. *WBC* white blood cell counts, *Ht* hematocrit, *Plt* platelet cell counts

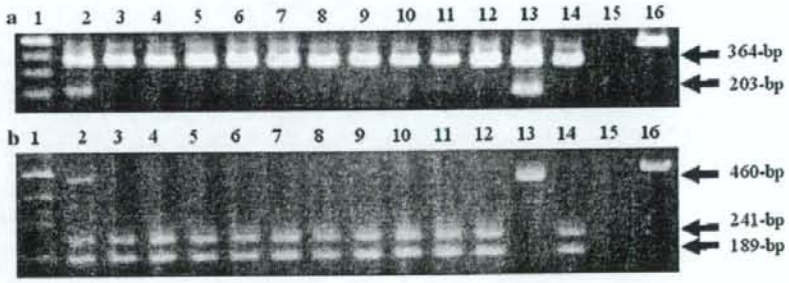

Fig. 2 Allele-specific PCR and restriction enzyme-based assessment of the *JAK2* V617F mutation in IE. **a** Presence of the *lower band* (203-bp product) indicates that the mutation is carried by the patient; the *upper band* (364-bp product) acts as an internal PCR control. *Lane 1* 100-bp marker, lane 2 IE No. 1, lane 3 IE No. 2, *lane 4* IE No. 3, *lane 5* IE No. 4, *lane 6* IE No. 5, *lane 7* IE No. 6, *lane 8* IE No. 7, *lane 9* IE No. 8, *lane 10* IE No. 9, *lane 11* IE No. 10, *lane 12* IE No. 11, *lane 13* HEL, *lane 14* HL-60, *lane 15* water, *lane 16* 500-bp marker. Aberrant bands were observed in only one IE patient (*line 2*, IE No. 1) and positive control (*line 13*, HEL). **b** Restriction enzyme-based assessment of the *JAK2* V617F mutation. Undigested bands (460-bp) were detected in *lane 2* and *lane 13*. The wild type allele was divided to 241-bp, 189-bp and 30-bp fragments. *Lane 1*100-bp marker, *lane 2* IE No. 1, *lane 3* IE No. 2, *lane 4* IE No. 3, *lane 5* IE No. 4, *lane 6* IE No. 5, *lane 7* IE No. 6, *lane 8* IE No. 7, *lane 9* IE No. 8, *lane 10* IE No. 9, *lane 11* IE No. 10, *lane 12* IE No. 11, *lane 13* HEL, *lane 14* HL-60; *lane 15* water, *lane 16* 500-bp marker

V617F mutation (Fig. 2b). The mutant allele was detected as an undigested form (460-bp), whereas the wild type allele was divided into 241, 189, and 30-bp fragments after digestion with *Bsa*XI. The V617F mutation was also detected in one of the 11 patients with IE (IE No.1) and all of the 15 PV patients (Table 2).

We next performed direct sequencing of the samples from 11 IE patients and two PV patients. Representative results are shown in Fig. 3a. The nucleotide change from C to A (reverse direction), corresponding to the *JAK2* V617F mutation, was clearly detected in PV (No. 3) and HEL. By contrast, there was no mutation detected by direct sequencing in samples from ten of the 11 IE patients. In the remaining one IE patient (IE No. 1) with aberrant bands by allele-specific PCR, the nucleotide change was not clearly detected by direct sequencing, but a faint green signal (nucleotide "A") was concurrently observed. To detect a small proportion of the mutation-positive cells, sequence

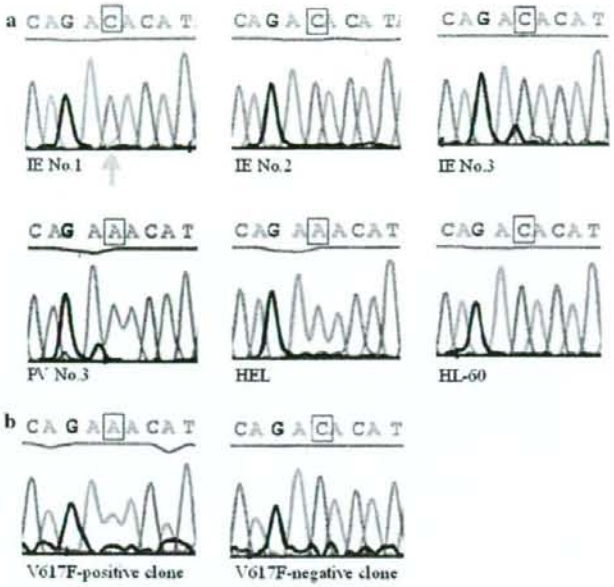

Fig. 3 Sequencing of the *JAK2* gene in erythrocytosis. **a** Direct sequencing was performed in IE, PV and leukemic cell lines. The nucleotide change from C to A (*reverse direction*), corresponding to *JAK2* V617F mutation, was clearly detected in PV No. 3 and HEL. **b** V617F-positive clone is detected in IE No. 1 (*left panel*) and V617F-negative clone is shown in the *right panel*

analysis was performed using plasmid clones containing the *JAK2* gene from IE No. 1. The V617F mutation was detected in four of 29 clones (14.0%) (Fig. 3b).

Since peripheral blood samples do not contain erythroblasts DNA, we used DNA from bone marrow smear samples. However, the *JAK2* V617F mutation was not detectable by allele-specific PCR in bone marrow samples from six IE (Table 2).

To determine the relevance of the *JAK2* mutations other than V617F, we also performed direct sequencing of exon 12. There was no mutation detected in all 11 IE (data not shown).

4 Discussion

The JAK2 V617F mutation was detected in one of the 11 IE patients by allele-specific PCR. The results of restriction enzyme-based assessment were concordant with those of allele-specific PCR. The present results show that the *JAK2* V617F mutation is a rare event in IE. This is apparently different from that of PV, since the *JAK2* V617F mutation was detected in all 15 samples from PV patients in our study. Percy et al. [16] reported that only one of 73 patients with erythrocytosis had the *JAK2* V617F mutation. However, Rossi et al. [17] reported that none of 11 IE had the *JAK2* V617F mutation. Our results indicated that the *JAK2* V617 mutation is rare in IE, differing from the incidence in PV.

In the V617F-positive IE patient, the *JAK2* mutation was subsequently analyzed by sequencing. A small proportion of mutation-positive cells (14.0%) were detected using independent plasmid clones, while the mutation was not clearly observed by direct sequencing. This difference is probably due to the sensitivity of these methods. It is generally considered that the sensitivity of direct sequencing is approximately 10% and that of allele-specific PCR is 2–3%. Proportion of mutation-positive cells of IE No. 1 was much smaller than that of PV. In this patient, his platelet counts were gradually increased over $40 \times 10^4/\mu L$ during observation around the examination (Fig. 1a). This patient might show progression to PV according to the new WHO diagnostic criteria proposed in 2007 [6], although the leukocyte count was within the normal range and splenomegaly was absent. In contrast, none of the remaining ten IE patients (V617F-negative) progressed to PV during long-term observation (median follow up: 6.6 years) from diagnosis to the most recent examination. The absence of the V617F mutation in bone marrow cells suggested that the mutation does not involve the erythroid lineage in these IE patients.

Previous longitudinal studies have reported that patients initially presenting with IE might show hematological evolution and clinical features allowing them to be reclassified as having PV [10, 18–20]. Najean et al. [10] reported that 10% of patients diagnosed as having pure erythrocytosis at initial presentation, progressed to PV at the late stage of the clinical course. In these studies, it was

unknown whether patients who progressed from IE to PV had the *JAK2* V617F mutation.

More recently, Scott et al. and Williams et al. [15, 21] reported that the novel *JAK2* mutations in exon 12 and *MPL* gene mutations were detected in *JAK2* V617F-negative PV and IE. Therefore, we performed direct sequence analysis on exon 12 of the *JAK2* gene, and there was no mutation detected in any of the 11 IE patients. The previous papers as well as our findings suggest that IE is a heterogeneous disorder.

In conclusion, *JAK2* V617F mutation is a rare event in IE in contrast to the incidence of PV. The majority of IE patients may have a genetic lesion different from PV, and the molecular mechanism responsible for IE remains unclear. With respect to the V617F mutation, IE may not be the first stage of PV. However, in our study, a small proportion of V617F mutation-positive cells were detected in one patient with IE. A further longitudinal study monitoring V617F positive-cells will clarify the process of progression from IE to PV in such a patient.

Acknowledgments This work was supported in part by a grant-in-aid from the International Research and Educational Institute for Integrated Medical Sciences (IREIIMS) of Tokyo Women's Medical University. We would like to thank Mr. Yukihiro Horie and Miss Mizuho Fukusaki for the preparation of blood specimens.

References

1. Ihle JN, Gilliland DG. Jak2: normal function and role in hemotopoietic disorders. Curr Opin Genet Dev. 2007;17:8–14.
2. Baxter EJ, Scott LM, Cambell PJ, et al. Acquired mutation of tyrosine kinase JAK2 in human myeloproliferative disorders. Lancet. 2005;365:1054–61.
3. Kralovics R, Passamonti F, Buser AS, et al. A gain-of-function mutation of JAK2 in myeloploliferative disorders. N Engl J Med. 2005;352:1779–90.
4. Cambell PJ, Scott LM, Buck G, et al. Definition of subtypes of essential thrombocythaemia and relation to polythaemia vera based JAK2 V617F muatation status: a prospective study. Lancet. 2005;366:1945–53.
5. Levine RL, Wadleigh M, Cool J, et al. Activating mutation in the tyrosine kinase JAK2 in polycythemia vera, essential thrombocythemia and myeloid metaplasia with myelofibrosis. Cancer Cell. 2005;7:387–97.
6. Tefferi A, Thiele J, Orazi A, et al. Proposals and rationale for revision of the world health organization diagnostic criteria for polycythemia vera, essential thrombocythemia, and primary myelofibrosis: recommendations from an ad hoc international expert panel. Blood. 2007;110:1092–7.
7. McMuillin MF, Bareford D, Cambell P, et al. Guidelines for diagnosis, investigation and management of polycythaemia/erythrocytosis. Br J Haematol. 2005;130:174–95.
8. Finazzi G, Gregg XT, Barbui T, et al. Idiopathic erythrocytosis and other non-clonal polycythemias. Best Pract Res Cl Hal. 2006;19:471–82.
9. Blacklock HA, Royle GA. Idiopathic erythrocytosis—a declining entity. Br J Haematol. 2001;115:774–81.
10. Najean Y, Triebel F, Dresch C. Pure erythrocytosis: reappraisal of study of 51 cases. Am J Hematol. 1981;10:129–36.
11. Michiels IJ, Barbui T, Finazzi G, et al. Diagnosis and treatment of polycythemia vera and possible future study designs of the PVSG. Leuk Lymphoma. 2000;36:239–53.
12. Murphy S, Petersen P, Iland H, et al. Experience of the Polycythemia Vera study group with essential thrombocythemia: a final report on diagnostic criteria, suvival and leukemic transition by treatment. Semin Hematol. 1997;34:29–39.
13. Pierre R, Imbert M, Thiele J, et al. *Polycythaemia vera WHO* classification of tumors, tumors of hematopietic and lymphoid tissues. Lyon: IARC Press; 2001. p. 32–4.
14. Woodman RC, Reinhardt P, Kanwar S, et al. Effects of human neutrophil elastase (HNE) on neutrophil function function in vitro and in inflamed microvessels. Blood. 1993;82:2188–95.
15. Scott LM, Tong W, Levine RL, et al. JAK2 exon 12 mutations in polycythrmia vera and idiopathephic erythrocytosis. N Engl J Med. 2007;356:459–68.
16. Percy MJ, Jones FGC, Green AR, et al. The incidence of the JAK2 V617F mutation in patients with idiopathic erythrocytosis. Hematologica. 2006;91:413–4.
17. Rossi D, Cortini F, Deambrogi C, et al. Usefulness of JAK2V617F mutation in distinguishing idiopathic erythrocytosis from polycythemia. Leuk Res. 2007;31:97–101.
18. Modan B, Modan M. Benign erythrocytosis. British J Haematol. 1968;14:375–81.
19. Pearson TC, Wethereley MG. The course and complications of idiopathic erythrocytosis. Clin Lab Hematol. 1979;1:189–96.
20. Finazzi G, Ruggeri M, Marconi M, et al. The natural history of idiopathic erythrocytosis: a cohort study of 74 patients. Blood. 2004;104:421a
21. Williams DM, Kim AH, Rogers O, et al. Phenotypic variations and new mutations in JAK2 V617F-negative polycythemia vera, erythrocytosis, and idiopathic myelofibrosis. Exp Hematol. 2007;35:1641–6.

Genetics and Molecular Biology, 31, 2, 427-430 (2008)

www.sbg.org.br

Short Communication

Infrequent V617F mutation of the *JAK2* gene in myeloid leukemia and its absence in lymphoid malignancies in Japan

Naoki Mori[1], Kentaro Yoshinaga[1], Makiko Tada[1,2], Yanhua Wang[1], Masayuki Shiseki[1] and Toshiko Motoji[1]

[1]*Department of Hematology, Tokyo Women's Medical University, Tokyo, Japan.*
[2]*Meiji Pharmaceutical University, Tokyo, Japan.*

Abstract

A unique mutation of the *JAK2* gene, V617F, has recently been identified in polycythemia vera, essential thrombocythemia and myeloid metaplasia with myelofibrosis. To determine the relevance of this mutation in other types of hematological neoplasms in Japan, we performed allele-specific polymerase chain reaction analysis on the *JAK2* gene. The V617F mutation was detected in one out of 130 myeloid neoplasms, but in none of 114 lymphoid malignancies and four biphenotypic acute leukemias. Although a favorable chromosomal alteration t(8;21)(q22;q22) was observed in one acute myeloid leukemia (AML) patient with the mutation, two courses of chemotherapy resulted in induction failure and short survival. Sequencing of *JAK2* cDNA revealed expression of the mutant allele in the patient. The V617F mutation might play a role in the pathogenesis of certain AML cases.

Key words: JAK2 gene, V617F mutation, signal transduction, acute myeloid leukemia, lymphoid malignancies.

Received: June 1, 2007; Accepted: December 14, 2007.

Myeloproliferative disorders (MPD) comprise a heterogeneous group of diseases including chronic myelocytic leukemia (CML), polycythemia vera (PV), essential thrombocythemia (ET), and myeloid metaplasia with myelofibrosis (MMM). With the exception of CML, characterized by the Philadelphia chromosome and the *BCR-ABL* fusion gene, genetic events causing these disorders have remained unidentified for a long time. The *Janus kinase 2 (JAK2)* gene encodes a tyrosine kinase involved in cytokine signal transduction. JAK phosphorylates cytoplasmic targets including signal transducers and activators of transcription (STAT). In hematological neoplasms, several chromosomal translocations involving the *JAK2* gene locus have been identified (Khwaja, 2006). Recently, a unique mutation of the *JAK2* gene, G to T transversion at nucleotide 1849 resulting in valine to phenylalanine substitution at amino acid position 617 (V617F), has been identified in MPD (Baxter *et al.*, 2005; James *et al.*, 2005; Kralovics *et al.*, 2005; Levine *et al.*, 2005a). This mutation was present in most patients with PV and in half of the patients with ET and MMM. Since the V617F mutation is located in the JH2 negative regulatory domain of the *JAK2* gene, it disrupts the auto-inhibitory activity of JAK2. In consequence, the mutation leads to constitutive tyrosine phosphorylation activity, promoting cytokine hypersensitivity and inducing erythrocytosis in a mouse model (James *et al.*, 2005).

Send correspondence to Naoki Mori. Department of Hematology, Tokyo Women's Medical University, 8-1 Kawada-cho, 162-8666 Shinjuku-ku, Tokyo, Japan. E-mail: mori@dh.twmu.ac.jp.

Recent studies have shown the V617F mutation to be present in some cases of acute myeloid leukemia (AML), myelodysplastic syndrome (MDS) and chronic myelomonocytic leukemia (CMMoL) (Jelinek *et al.*, 2005; Levine *et al.*, 2005b). However, limited information is available to determine whether the mutation is specifically associated with myeloid neoplasms, and most of the studies are from Europe and North America. In order to assess the range and frequency of the mutation in Japanese patients with hematological neoplasms, we performed allele-specific polymerase chain reaction (PCR) analysis on the *JAK2* gene.

Bone marrow, peripheral blood or lymph node samples from 248 hematological neoplasms were analyzed after obtaining written informed consent (Table 1). Of the 248 samples, 130 were myeloid neoplasms, 114 were lymphoid neoplasms, and four were biphenotypic acute leukemias (BAL). The current study was conducted within the guidelines and with the approval of the institutional review board. The primer sequences for allele-specific PCR were previously published (Baxter *et al.*, 2005):

ALLF-S, 5'-AGCATTTGGTTTTAAATTATGGAGTATATT-3';

ALLF-IC, 5'-ATCTATAGTCATGCTGAAAGTAGGAGAAAG-3'; and

Table 1 - *JAK2* V617F mutations in hematological neoplasms.

	Number of samples	Number of V617F myeloid malignancies
Myeloid malignancies		
AML	38	1
MDS	38	0
RAEB-t[1]	2	0
MDS/AML	16	0
CML CP[2]	18	0
CML AP[3]	1	0
CML BC[4]	11	0
CMMoL	5	0
aCML[5]	1	0
Lymphoid malignancies		
MM	48	0
MGUS[6]	2	0
ALL	40	0
CLL	7	0
ML	8	0
Macroglobulinemia	2	0
ATL	7	0
Biphenotypic acute leukemia	4	0
Total	248	1

[1]RAEB-t, refractory anemia with excess of blasts in transformation; [2]CP, chronic phase; [3]AP, accelerated phase; [4]BC, blast crisis; [5]aCML, atypical chronic myeloid leukemia; [6]MGUS, monoclonal gammopathy with undetermined significance.

ALLR-S, 5'-CTGAATAGTCCTACAGTGTTTTC AGTTTCA-3'.

ALLF-S is specific for the mutant allele and contains an intentional mismatch at the third nucleotide from the 3' end, to improve specificity. After 5 min at 94 °C, 36 amplification cycles of 60 s at 94 °C, 60 s at 58 °C and 60 s at 72 °C were performed, with a subsequent 7 min extension at 72 °C. Electrophoresis was repeated two or three times in each sample, using independent PCR products. Primers ALLF-S and ALLR-S amplify 203-bp (base pair) products, while the size of products using primers ALLF-IC and ALLR-S is 364 bp. The 203-bp products indicated the V617F mutation, while the 364-bp products indicated the internal control. PV samples with the V617F mutation were used as positive control. Aberrant bands were detected in one of the 248 samples (AML02, Figure 1 lane 5).

To confirm the aberrant bands detected by allele-specific PCR, DNA from AML02 was subsequently sequenced in both directions on a MegaBase sequence system (Amersham, Buckingham, UK). PCR products were purified and ligated into pGEM-T vector (Promega, Madison, WI, USA). Sequencing revealed G to T transversion at nucleotide 1849, resulting in the V617F mutation (Figure 2). Several samples without aberrant bands by allele-specific

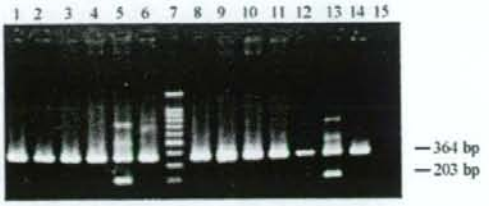

Figure 1 - Allele-specific PCR analysis of the *JAK2* gene in hematological neoplasms. Ten of 20 µL of PCR products were separated by electrophoresis on 2% agarose gel, stained with ethidium bromide and visualized by ultraviolet illumination. The size of the products is indicated on the right. Aberrant bands were detected in one of the AML samples (lane 5). Lane 1, AML01; lane 2, MDS01; lane 3, ALL01; lane 4, BAL01; lane 5, AML02; lane 6, AML03; lane 7, 100 bp ladder; Lane 8, ALL02; lane 9, AML04; lane 10, AML05; lane 11, AML06; lane 12, CLL01, lane 13, PV01; lane 14, CML01, lane 15, water. Aberrant bands of PV01 are shown as positive control (lane 13).

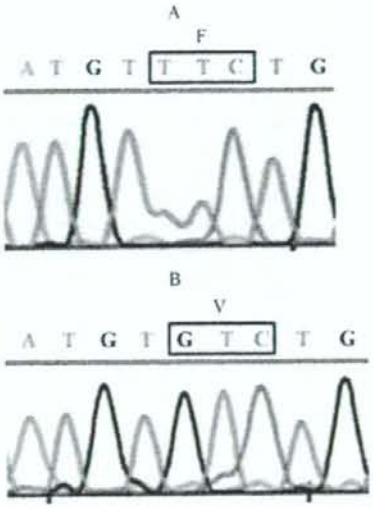

Figure 2 - Sequence analysis of the *JAK2* gene in AML. Sequencing identified G to T transversion at nucleotide 1849, resulting in the V617F mutation in the AML sample (A, AML02). Wild-type sequences are shown as control (B, MM01).

PCR were also sequenced, but only wild-type sequences were obtained.

To determine the expression of the JAK2 V617F mutation, we performed reverse transcriptase-PCR (RT-PCR) analysis in AML02 (Mori *et al.*, 1990). The following sequences were used for the primers: RT-11F1, 5'-AAAGC CTTGGCCAAGGCACTT-3'; and RT-13R2, 5'-ATGCA TGGCCCATGCCAACTG-3'. After 5 min at 94 °C, 30 amplification cycles of 60 s at 94 °C, 60 s at 55 °C and 60 s at 72 °C were performed, with a subsequent 10 min extension at 72 °C. Primers RT-11F1 and RT-13R2 amplify

340-bp products. Sequencing of *JAK2* cDNA revealed the expression of the mutant allele in 20 out of 41 AML02 clones.

The V617F mutation of the *JAK2* gene was found in one of the 130 myeloid neoplasms, but not in the 114 lymphoid malignancies or in the four biphenotypic acute leukemias. The mutation was detected in the majority of Japanese patients with PV and ET (K Yoshinaga, N Mori, Y Wang, M Shiseki, T Motoji, unpublished data). In contrast to classic MPD, the V617F mutation was infrequent in myeloid leukemia and absent in lymphoid malignancies. Recent reports show that the JAK2 V617F mutation was not identified in either acute lymphoblastic leukemia (ALL) or chronic lymphocytic leukemia (CLL) (Levine *et al.*, 2005b). Our study showed that also in Japan the V617F mutation is absent in ALL and CLL. Furthermore, it was also undetectable in adult T-cell leukemia (ATL), macroglobulinemia, multiple myeloma (MM), and malignant lymphoma (ML).

AML02 was obtained from a patient with AML showing M2 morphology according to the French-American-British (FAB) classification at diagnosis. This patient was a 70-year-old woman with no history of preceding MPD or MDS. Peripheral blood tests revealed 50.1 x 10^9/L leukocytes with 76.5% blast cells, 7.8 g/dL hemoglobin, and 55 x10^9/L platelets. Although the favorable chromosomal alteration t(8;21)(q22;q22) accompanied by *AML1/ETO* transcripts was the only chromosomal abnormality observed in the patient, two courses of chemotherapy resulted in induction failure and short survival. The mutation was found in nine out of 14 AML02 clones. Since this sample was expected to contain more than 90% blast cells after mononuclear cell isolation, this case may have been heterozygous for the V617F mutation. Another possibility is that a substantial proportion of the leukemic cells from AML02 did not harbor the mutation.

The V617F mutation was detected in one of the 38 patients with AML (3%). Other recent studies found a similar incidence of the V617F mutation: 0/17 (Jones *et al.*, 2005), 5/90 (6%) (Scott *et al.*, 2005), 2/39 (5%) (Jelinek *et al.*, 2005), 4/222 (2%, three had preceding MPD) (Levine *et al.*, 2005b), 1/152 (0.7%) (Frohling *et al.*, 2006), and 2/112 (2%) (Lee *et al.*, 2006). The V617F mutation in AML was initially found in FAB M6 (1/53) (Frohling *et al.*, 2006) and FAB M7 (2/11) (Jelinek *et al.*, 2005), while the FAB subtype of AML was not described in other reports. In the current study, this mutation was also found to be present in one out of 12 patients with AML M2 (8%): one of the four patients with t(8;21)(q22;q22). After submission of our paper, expression of the JAK2 V617F mutation was reported in two out of 18 MDS/AML but not in 198 *de novo* AML cases (Nishii *et al.*, 2007). In contrast to their result, in the present study expression of the mutant allele was detected in AML02, as described above.

Our study revealed that the V617F mutation is infrequent in myeloid leukemia and absent in lymphoid malignancies in Japan. Nevertheless, it was detected in AML02, along with the favorable cytogenetic alteration t(8;21)(q22;q22). Previous studies have demonstrated that additional event(s) are required for the development of AML in the presence of t(8;21)(q22;q22) (Yuan *et al.*, 2001; Kuchenbauer *et al.*, 2006). Tyrosine kinases have been involved in several disorders including BCR-ABL in CML, PDGFRβ in CMMoL, and PDGFRα in chronic eosinophilic leukemia. Furthermore, activating mutations in the *FLT3* receptor tyrosine kinase gene are the most common genetic events in AML. Patients with FLT3 mutations have a poor prognosis, suggesting the important role of tyrosine kinase gene mutations in leukemogenesis. The relation between the V617F mutation and short survival in AML02 is unclear. The V617F mutation might confer a proliferative advantage to blast cells and play a role in the pathogenesis of certain AML cases. As suggested for FLT3 mutations, constitutive signaling in the absence of ligand may result in reduced apoptosis of the leukemic cells or may grant increased repair capacity following cell damage; either of these mechanisms could be considered as inducing chemoresistance (Kottaridis *et al.*, 2001). Further studies will clarify the incidence and significance of the V617F mutation in AML with t(8;21)(q22;q22).

References

Baxter EJ, Scott LM, Campbell PJ, East C, Fourouclas N, Swanton S, Vassiliou GS, Bench AJ, Boyd EM, Curtin N *et al.* (2005) Acquired mutation of the tyrosine kinase JAK2 in human myeloproliferative disorders. Lancet 365:1054-1061.

Frohling S, Lipka DB, Kayser S, Scholl C, Schlenk RF, Dohner H, Gilliland DG, Levine RL and Dohner K (2006) Rare occurrence of the *JAK2* V617F mutation in AML subtypes M5, M6, and M7. Blood 107:1242-1243.

James C, Ugo V, Le Couédic J-P, Staerk J, Delhommeau F, Lacout C, Garçon L, Raslova H, Berger R, Bennaceur-Griscelli A *et al.* (2005) A unique clonal *JAK2* mutation leading to constitutive signaling causes polycythaemia vera. Nature 434:1144-1148.

Jelinek J, Oki Y, Gharibyan V, Bueso-Ramos C, Prchal JT, Verstovsek S, Beran M, Estey E, Kantarjian HM and Issa J-PJ (2005) *JAK2* mutation 1849G > T is rare in acute leukemias but can be found in CMML, Philadelphia chromosome-negative CML, and megakaryocytic leukemia. Blood 106:3370-3373.

Jones AV, Kreil S, Zoi K, Waghorn K, Curtis C, Zhang L, Score J, Seear R, Chase AJ, Grand FH *et al.* (2005) Widespread occurrence of the *JAK2* V617F mutation in chronic myeloproliferative disorders. Blood 106:2162-2168.

Khwaja A (2006) The role of Janus kinases in haemopoiesis and haematological malignancy. Br J Haematol 134:366-384.

Kottaridis PD, Gale RE, Frew ME, Harrison G, Langabeer SE, Belton AA, Walker H, Wheatley K, Bowen DT, Burnett AK *et al.* (2001) The presence of a FLT3 internal tandem dupli-